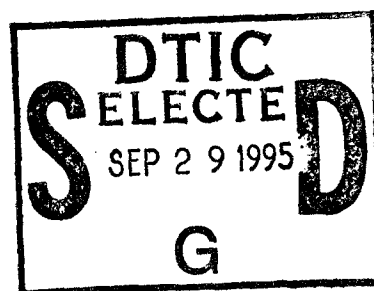


A TRIDENT SCHOLAR PROJECT REPORT

NO. 231

20
"The Design and Construction of a High Temperature
Photon Emitter for a Thermophotovoltaic Generator"



19950927 149

UNITED STATES NAVAL ACADEMY
ANNAPOLIS, MARYLAND

This document has been approved for public
release and sale; its distribution is unlimited.

DTIC QUALITY INSPECTED 5

REPORT DOCUMENTATION PAGE			Form Approved OMB no. 0704-0188	
<small>Public reporting burden for this collection of information is estimated to average 1 hour of response, including the time for reviewing instructions, searching existing data sources, gathering and maintaining the data needed, and completing and reviewing the collection of information. Send comments regarding this burden estimate or any other aspect of this collection of information, including suggestions for reducing this burden, to Washington Headquarters Services, Directorate for Information Operations and Reports, 1215 Jefferson Davis Highway, Suite 1204, Arlington, VA 22202-4302, and to the Office of Management and Budget, Paperwork Reduction Project (0704-0188), Washington DC 20503.</small>				
1. AGENCY USE ONLY (Leave blank)		2. REPORT DATE 9 May 1995		3. REPORT TYPE AND DATES COVERED
4. TITLE AND SUBTITLE The design and construction of a high temperature photon emitter for a thermophotovoltaic generator				5. FUNDING NUMBERS
6. AUTHOR(S) Robert S. McHenry				
7. PERFORMING ORGANIZATIONS NAME(S) AND ADDRESS(ES) U.S. Naval Academy, Annapolis, MD				8. PERFORMING ORGANIZATION REPORT NUMBER USNA Trident report; no. 231 (1995)
9. SPONSORING/MONITORING AGENCY NAME(S) AND ADDRESS(ES)				10. SPONSORING/MONITORING AGENCY REPORT NUMBER
11. SUPPLEMENTARY NOTES Accepted by the U.S. Trident Scholar Committee				
12a. DISTRIBUTION/AVAILABILITY STATEMENT This document has been approved for public release; its distribution is UNLIMITED.				12b. DISTRIBUTION CODE
13. ABSTRACT (Maximum 200 words) This report documents the engineering design of a high temperature photon emission core for a thermophotovoltaic (TPV) electrical generator. A comprehensive design approach included theoretical research, computer modeling, prototype experimentation, and final system design. The designed photon emitting surface was a 12 inch long, 4 inch diameter cylinder which produced a near blackbody photon spectrum centered at 0.7 eV. The emitter was heated by methane combustion and could achieve temperatures in excess of 2700°F. Ceramic materials, including inexpensive ceramic mortars, were utilized for the majority of the system components. The design included a simple recuperative heat exchanger to preheat combustion air and set point gas flow control to maintain steady state emission temperatures. The project was conducted as part of the Trident Scholar Program at the United States Naval Academy by interagency agreement with the Department of Energy.				
14. SUBJECT TERMS ceramic, combustor, emitter, photon, recuperation, thermophotovoltaic				15. NUMBER OF PAGES
				16. PRICE CODE
17. SECURITY CLASSIFICATION OF REPORT UNCLASSIFIED	18. SECURITY CLASSIFICATION OF THIS PAGE UNCLASSIFIED	19. SECURITY CLASSIFICATION OF ABSTRACT UNCLASSIFIED	20. LIMITATION OF ABSTRACT UNCLASSIFIED	

"The Design and Construction of a High Temperature Photon Emitter for a Thermophotovoltaic Generator"

by

Midshipman Robert S. McHenry, Class of 1995
United States Naval Academy
Annapolis, Maryland

Robert S. McHenry

Certification of Advisers Approval

Assistant Professor Mark J. Harper
Department of Naval Architecture, Ocean and Marine Engineering

Mark J. Harper

23 MAY 95

Associate Professor Keith W. Lindler
Department of Naval Architecture,
Ocean and Marine Engineering

Keith W. Lindler

5/11/95

Professor Martin E. Nelson
Department of Naval Architecture,
Ocean and Marine Engineering

Mart E Nelson

5/11/95

Acceptance for the Trident Scholar Committee

Associate Professor Joyce E. Shade
Chair, Trident Scholar Committee

Joyce E. Shade

19 May 95

ABSTRACT

This report documents the engineering design of a high temperature photon emission core for a thermophotovoltaic (TPV) electrical generator. A comprehensive design approach included theoretical research, computer modeling, prototype experimentation, and final system design. The designed photon emitting surface was a 12 inch long, 4 inch diameter cylinder which produced a near blackbody photon spectrum centered at 0.7 eV. The emitter was heated by methane combustion and could achieve temperatures in excess of 2700°F. Ceramic materials, including inexpensive ceramic mortars, were utilized for the majority of the system components. The design included a simple recuperative heat exchanger to preheat combustion air and set point gas flow control to maintain steady state emission temperatures. The project was conducted as part of the Trident Scholar Program at the United States Naval Academy by interagency agreement with the Department of Energy.

KEYWORDS: ceramic, combustor, emitter, photon, recuperation, thermophotovoltaic

Accession For	
NTIS CRA&I	<input checked="" type="checkbox"/>
DTIC TAB	<input type="checkbox"/>
Unannounced	<input type="checkbox"/>
Justification _____	
By _____	
Distribution /	
Availability Codes	
Dist	Avail and/or Special
A-1	

TABLE OF CONTENTS

Abstract	1
Table of Contents	2
List of Figures	4
List of Tables	5
Nomenclature	6
1.0 INTRODUCTION	8
1.1 Impetus	8
1.2 Objectives	8
1.3 Methodology	9
2.0 BACKGROUND	10
2.1 The Thermophotovoltaic Process	10
2.2 History	11
2.3 Advantages	12
2.4 Applications	13
3.0 PHASE I — SUPPORTING RESEARCH	18
3.1 Photonic Processes	18
3.2 Combustion	21
3.3 Materials	23
4.0 PHASE II — SYSTEM MODELING	27
4.1 Mathematical Relationships	27
4.2 Computer Modeling	31

TABLE OF CONTENTS (Continued)

5.0	PHASE III — PROTOTYPING	36
5.1	Design	36
5.2	System Construction	39
5.3	Prototype Operation	40
5.4	Experimentation	44
6.0	PHASE IV — FINAL DESIGN	47
6.1	Combustor Design	47
6.2	Balance of Plant Requirements	49
7.0	CONCLUSIONS	53
7.1	Design Evaluation	53
7.2	Project Results	55
7.3	Project Conclusions	55
	References	57
	Appendix	60

LIST OF FIGURES

<u>FIGURE #</u>	<u>TITLE</u>	<u>PAGE</u>
2-1	TPV System Schematic	11
2-2	TPV Solar Concentrator	15
2-3	Nuclear TPV System	15
2-4	TPV Gas Turbine Cogeneration	17
3-1	Blackbody Emissive Power	19
3-2	TPV Cell	20
3-3	Characteristics of Combustor Types	22
4-1	Combustor Heat Balance	30
4-2	Data Input Page	33
4-3	Radiation Heat Transfer Page	34
4-4	Evolutionary Model Development	35
5-1	Prototype Design	38
5-2	Complete System Schematic	39
5-3	TPV Burner Prototype	41
5-4	Experimental Exhaust Temperature	44
5-5	Experimental Temperature Profile	45
5-6	Combustor Efficiency Curve Fitting	46
6-1	Predicted Emitter Temperature Profile	48
6-2	Final TPV Combustor Design	50
6-3	Heat Exchanger Design	51

LIST OF TABLES

<u>TABLE #</u>	<u>TITLE</u>	<u>PAGE</u>
2-1	Possible TPV Applications	14
3-1	Physical Laws of Photon Emission	18
3-2	Lower Heating Value and Flame Temperature of Fuels	21
3-3	Material Characteristics	23
3-4	Typical Characteristics of Ceramics	24
3-5	Primary Ceramic Candidates	25
4-1	Fluid Flow Equations	27
4-2	Methane Combustion Reactions	28
4-3	Basic Heat Transfer Equations	31
4-4	Computer Model "Pages"	32
7-1	Complete Design Specifications	53
7-2	Evaluation of Initial Objectives	54

NOMENCLATURE

A	Flow area in inches ² .
α	Absorptivity: a numerical value between zero and one, which characterizes the ratio of incident energy absorbed by a material to incident energy reflected or transmitted.
c	Speed of light: 9.84×10^8 ft/sec.
C_1	First radiation constant: 1.1870×10^8 Btu/ μ^4 /hr ft ² .
C_2	Second radiation constant: 2.5896×10^4 μ° R.
D	Hydraulic diameter: four times the flow cross-sectional area over the wetted perimeter.
ϵ	Emissivity: the ratio of the incident energy absorbed by an actual body to the incident energy absorbed by an ideal blackbody with $\alpha = 1$.
E_b	Blackbody emissive power: the radiative power of a blackbody emitter as a function of photon wavelength in W/m ² μ .
e_p	Photon energy: the energy possessed by a single photon in eV.
eV	Electron volt: 1.602×10^{-19} Joules.
F	Radiative view factor: a numerical value between zero and one defined by the ratio of radiated energy emitted and received by two bodies.
g	Gravitational acceleration: 32.2 ft/sec ² .
g_c	Gravitational constant: 32.174 lbm ft / lbf sec ² .
h	Planck's constant: 6.6256×10^{-34} J-sec.
h_c	Convection heat transfer coefficient.
h_f	Head loss due to frictional flow.
k	Conduction heat transfer coefficient.

NOMENCLATURE (Continued)

L	Flow length in inches.
λ	Photon wavelength in μ .
λ_{\max}	Maximum wavelength within spectrum.
LHV	Lower Heating Value: the amount of heat liberated per unit mass of fuel.
\dot{m}	Mass flow rate in lbm/hr.
μ	Absolute viscosity in lbf sec / ft ² .
P	Pressure in psia.
R	Specific gas constant.
Re	Reynolds number: the ratio of the inertial forces to the viscous forces.
ρ	Density in lbm/ft ³
ρ	Reflectivity: a numerical value between zero and one, which characterizes the ratio of incident energy reflected away from a material to the incident energy absorbed or transmitted.
Q_c	Convective heat transfer
Q_k	Conductive heat transfer
Q_r	Radiative heat transfer
σ	Stefan-Boltzmann constant:
τ	Transmissivity: a numerical value between zero and one, which characterizes the ratio of incident energy transmitted through a material to the incident energy absorbed or reflected.
T	Temperature: °F
V	Velocity in ft/sec
ν	Frequency in Hz

1.0 SUMMARY

This was an engineering research and design project aimed at developing the photon emitting core of an operational thermophotovoltaic (TPV) generator. This paper outlines the specific requirements of the system, the methodology used to meet those requirements, and an analysis of the final results.

1.1 IMPETUS

This project was conducted under the auspices of the U.S. Naval Academy Trident Scholar Program in which well-qualified First Class Midshipmen are selected to accelerate their regular academic courses and complete advanced research work in their major field of study. The author of this report, Midshipman Robert S. McHenry, was accepted into the program for the 1994-1995 Academic Year from the Naval Architecture, Ocean and Marine Engineering Department.

The work completed in this project was conducted under the direction and funding of the Department of Energy (DOE) in accordance with Interagency Agreement DE-A112-94SN39277. As outlined in that agreement, the objective of the research was the complete development and design of an operational high temperature photon emission device to serve as the core of an independently designed thermophotovoltaic electrical generator.

1.2 OBJECTIVES

The above mentioned agreement dictated that the project produce an optimized design for a TPV photon emitter with the following characteristics:

1. Geometrically compatible with the DOE TPV generator system
2. Uniform 2700°F photon emission temperature
3. Near blackbody photon emission characteristics
4. Portable and completely self-sufficient design
5. Optimized cycle efficiency

In addition to this design, the scope of work also included the following research directives:

1. Optimal fuel selection
2. Gas burner design and optimization
3. Flame and temperature control
4. Thermally suitable system materials
5. Development of computer simulation software

1.3 METHODOLOGY

In accordance with Section 1.2, the objectives of the project were achieved through the following engineering design approach:

Phase I: Supporting Research A theoretical and literature-based review of the applicable system mechanics including photon emission, combustion processes and high temperature materials science.

Phase II: System Modeling Definition of the precise mathematical system of fluid mechanics, combustion chemistry and heat transfer, including a comprehensive computer-based model for use as a predictive design tool.

Phase III: Prototyping The design and construction of a prototype photon emitter system to gain operational experience and to facilitate the completion of an empirical validation analysis on the computer model.

Phase IV: Final Design Incorporation of prototype experience and computer model system optimization into a detailed engineering design for an operational TPV photon emitter that satisfies the initial objectives.

2.0 BACKGROUND

Thermophotovoltaic energy conversion is an electrical power generation process that converts thermal energy into electrical energy through photon coupling. Simply speaking, it is analogous to a solar power system in which the sun has been replaced by a man-made thermal source. This thermal source is used to heat an emitter that radiates infrared photons. The photons are collected in a photovoltaic diode where they are converted into a DC electrical current. This electrical generation process has the potential for high efficiency while exhibiting characteristics that may prove advantageous in a wide variety of military and commercial applications.

2.1 THE THERMOPHOTOVOLTAIC PROCESS

The thermophotovoltaic energy conversion process can be characterized by three distinct phases. (1) First is the emission of energetic photon radiation. A high temperature thermal source is required to induce photon radiation from the surface of a solid body. The photons are emitted with a wide spectrum of energies which can be shifted by varying the surface temperature of the emitter body. Efficient energy conversion and useful power outputs require that the peak of the emitted photon radiation coincide with the optimal photon energy for electrical conversion. (2) To optimize the coincidence of the emitted radiation to that optimal discrete photon energy, a selective spectral filter is used between the emitter and the photovoltaic diode. Such a filter must be designed so that it reflects all photons above and below the optimal photon energy back to the emitter where they can be reabsorbed and reemitted across the entire emission spectrum. (3) The narrow band of photons that are allowed to pass through the filter impinge on the photovoltaic diode to undergo a photoelectric reaction and generate electron-hole pairs within the diode crystal. The discrete photonic energy needed to generate an electron-hole pair determines the optimum energy band of photons selected by the spectral filter. By tuning the system in this way, theoretical conversion efficiencies as high as 60% can be achieved (Chubb, 1993).

Taken together, the photon emitter, spectral control filter, and photovoltaic semiconductor diode comprise the complete TPV concept shown in Figure 2-1 on page 11. The result is a generator that converts thermal energy to electricity without any intermediate working substance and without any moving parts, offering a number of advantages over conventional power generation methods as discussed in Section 2.3.

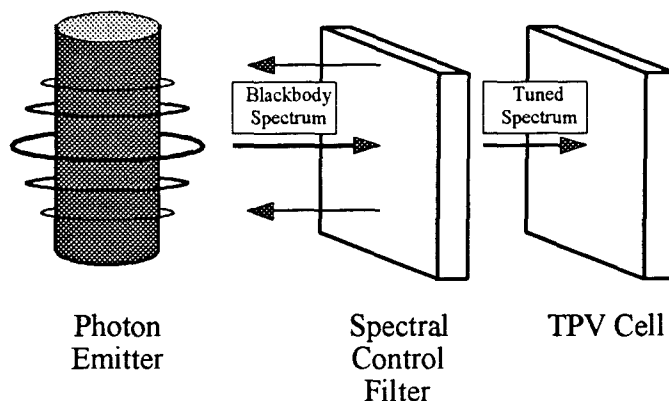


FIGURE 2-1: TPV System Schematic

2.2 HISTORY

The theoretical concept for TPV energy conversion systems can be traced back to a series of lectures at the Massachusetts Institute of Technology (MIT) in the early 1960's (Belkhat, 1993). Initial research at MIT spawned interest at other academic institutions as well as at the U.S. Army's Electronic Research Development Laboratory (Kittl, 1972). Throughout the 1960's and 1970's several projects were conducted to investigate both the high temperature emittance of suitable materials and the conversion efficiencies of current photovoltaic cells. While several designs were generated and analyzed during this time, the theoretical concept proved difficult to implement experimentally. The primary obstacles were the lack of suitable materials that could withstand the thermal stresses of high temperature operation and the inefficiency of the photon-to-electricity conversion process. Those TPV generators constructed were not competitive with conventional power generation methods.

While interest waned in the academic community, the government maintained several TPV research programs aimed at developing generators for specific applications such as satellite power sources and various military uses. The National Aeronautics and Space Administration's (NASA) Lewis Research Center contracted General Atomics to investigate nuclear powered TPV conversion in the early 1980's, resulting in the first design of a relatively large scale 184.7 kW generator (Belkhat, 1993). During the same period, developments in ceramic materials science and photovoltaic conversion efficiency offered hope for overcoming the initial obstacles and designing a cost effective TPV system. As interest in the area reemerged, a variety of novel designs and concepts arose offering several new approaches and applications.

By the early 1990's the technology had matured to the point that several companies developed and patented operational TPV units for incorporation into gas-fired home appliances. The Tecogen Company built a home furnace system featuring a TPV cogenerative unit capable of supplying all electrical needs for blowers and controls, while the Quantum Group did the same for a hot water heater (Block, 1992). More recently, the University of Washington has incorporated a TPV generator into their hybrid electrical vehicle program (Fritz, 1995). Several other patents have been submitted for TPV generators using techniques such as rotary bed combustion, fibrous emissive burners and solar concentration.

Today, efforts to improve the performance of TPV power generation units are being actively pursued in a number of major research venues. The government is funding research into large scale power generation in the Department of Energy (DOE), field portable generator units in the Army (Guazzoni, 1995) and NASA (Chubb, 1993), and marine applications in the Navy (Belkhat, 1993). Companies such as General Motors (GM) (Belkhat, 1993), General Electric (GE) (Guazzoni, 1995), the Gas Research Institute (GRI) (Coubrough, 1988, Kleiner, 1988 and Nelson, 1993), and the Electric Power Research Institute (EPRI) (Levy, 1979) have all funded projects at some level. With the maturity and breadth of developmental work accumulating and positive results being reported in a variety of studies, TPV technologies are in a position to become economically competitive in a wide range of commercial and military uses.

2.3 ADVANTAGES

The research history of the TPV process has spanned a wide range of applications and industries, indicating the versatility of the concept and the variety of inherent advantages that it offers. TPV systems consist of a direct energy conversion process, with only photonic coupling, eliminating the complexity, cost, and inefficiency associated with intermediate working substances. For example, consider the energy dynamics of a common steam boiler. Thermal energy is released from a fuel source and is absorbed by water where it is converted to the enthalpic state energy of steam. This steam is then passed through a nozzle where the enthalpic energy is converted to kinetic energy. The kinetic energy of the steam jet impinges upon the blades of a turbine and is partially converted to mechanical rotational energy. Finally, the rotational energy of the turbine shaft turns a generator and outputs electrical current. A TPV system involves only the generation and recovery of the photon radiation and therefore has higher efficiency potential and much simpler balance of plant engineering requirements (Belkhat, 1993).

The second advantage of the TPV generator concept is that it requires no moving parts. This has the direct result of lower maintenance and operational costs as well as simplification of plant design and support requirements. In a number of marine environment

and military applications, it also means a very quiet power source with a low acoustic signature (Belkhat, 1993). Such acoustic considerations are important for covert special forces power units and any undersea uses such as sonobuoys and submarine auxiliary power or propulsion. Due to the reduced balance of plant requirements and simple core designs, TPV systems also offer more power per unit weight than most competing conversion processes (Belkhat, 1993). This makes them particularly attractive for use in portable or weight sensitive equipment such as space probes, satellites, remote sensing stations, and sonobuoys. It also allows for greater endurance due to the increased fuel margin and it offers improvement in ship stability and design freedom when compared to diesel electric turbine sets for shipboard auxiliary electrical loads or primary electric propulsion (Apriainen, 1993). Finally, the virtual independence of the TPV conversion process from the type of thermal source used and the versatility of the system configuration allow for wide application as an addition to existing power generators. By incorporating TPV technology into current systems such as gas turbines or home furnaces, they can cogeneratively produce auxiliary power while operating solely on the previously wasted exhaust gas heat (Belkhat, 1993).

2.4 APPLICATIONS

The unique set of advantages inherent to the TPV conversion process, regardless of developed system efficiency, make the technology attractive for several specific areas of commercial and military use listed in Table 2-1 on page 14.

The commercial gas appliance industry has begun to develop and utilize cogenerative TPV units in their home appliances. These appliances utilize efficient clean combustion processes and develop flame temperatures up to 2700°F (Block, 1992). In most cases a large fraction of this high grade thermal energy is lost in the exhaust gases and offers the ideal situation for a TPV bottom cycle to generate electricity from the waste heat. With current operational efficiencies at approximately 20% (Duomarco, 1984), a relatively small array of photovoltaic cells can generate enough electricity to power the combustion blowers, solenoid valves and control systems while charging a storage battery for ignition in order to make the appliance completely independent of outside electrical hookup (Valenti, 1993). An example of the utility of such a system that actually spurred the procurement of cogenerative furnaces was the March 1991 ice storm that left nearly 200,000 Rochester Gas and Electric customers without power for up to two weeks. The majority of these homes had natural gas powered furnaces and water heaters but could not heat their homes or water due to the lack of electrical power for fans and pumps. The TPV cogenerative cycle would allow for continued operation at such times as well as reducing the daily electrical load of the household (Block, 1992). The same concept is also feasible on a larger scale for industrial heat processing, such as steel working or porcelain manufacture, where the TPV addition could power much or all of the plant's electrical load.

TABLE 2-1: Possible TPV Applications

★ COMMERCIAL APPLICATIONS	<ul style="list-style-type: none"> - Cogenerative Home Appliances - Hybrid Electric Vehicle - Satellite Power
★ LARGE SCALE POWER GENERATION	<ul style="list-style-type: none"> - Fossil Fuel - Nuclear - Solar Concentrator - Cogenerative / Bottom Cycle
★ SCIENTIFIC USES	<ul style="list-style-type: none"> - Deep Space Probe Power Units - Remote Sensing Stations
★ MARINE ENVIRONMENT	<ul style="list-style-type: none"> - Electric Ship Propulsion - Auxiliary Power Generation - Cogenerative Power
★ MILITARY DEFENSE	<ul style="list-style-type: none"> - Portable Power Unit - Special Forces Generator - Long Duration Sonobuoys - Ship and Submarine Propulsion - Power Cogeneration - Optical Laser Pump - Satellite Power

Current TPV efficiencies make it noncompetitive as a primary utility power generator, but the potential for significant advances in this area is great enough that several studies and designs have been completed. Due to the versatility of the TPV concept, it can be applied to any conventional fuel source including fossil fuel combustion, nuclear fission, and solar collection. Of these methods, the combustion powered and solar concentrator designs are the only viable options being developed at this time. Initial studies have been done regarding nuclear TPV, but requirements for radical reactor redesign in the nearly static nuclear industry, as well as estimates of high neutron damage to the TPV emitter and collecting cell components, have prevented further effort (Levy, 1979). The fossil fuel designs have been used for the small scale commercial applications outlined above but do not have efficiencies competitive with other combustion systems and therefore have not experienced any significant scale up efforts. The same cogenerative techniques discussed previously can be applied to almost all fossil fuel power plants resulting in increased plant efficiency by generating

additional electrical power from the waste heat exhaust. The solar TPV design has the greatest immediate potential to reach a mature development stage due to the fact that it offers increased efficiency over current solar arrays while reducing the environmentally and financially negative size of large scale solar power plants. By concentrating the sunlight in a parabolic reflector, the intensity is increased to the point that 30% cell efficiencies have been recorded as compared to nominal 10% efficiency in standard solar cells (Belkhat, 1993). Two conceptual designs of large scale TPV power converters for solar and nuclear fuel types are shown in Figure 2-2 and Figure 2-3 (Belkhat, 1993).

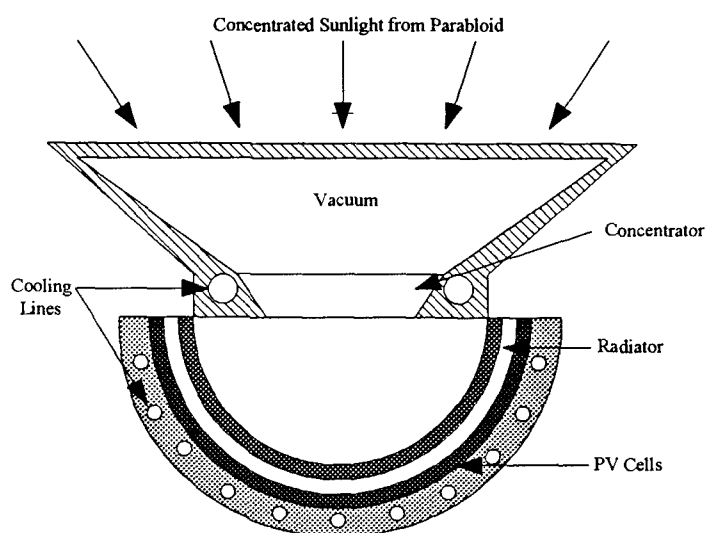


FIGURE 2-2: TPV Solar Concentrator

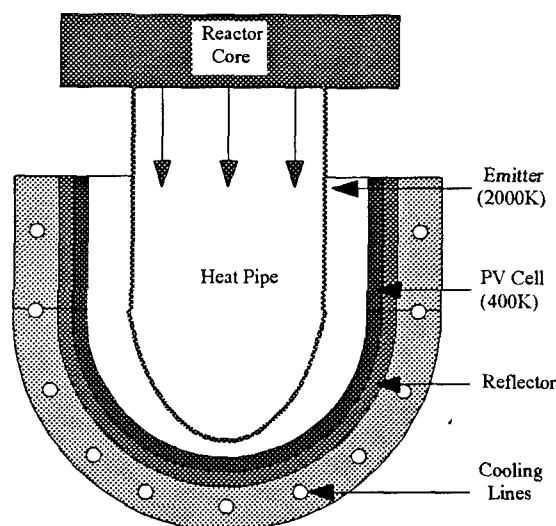


FIGURE 2-3: Nuclear TPV System

The scientific community has found several promising applications of TPV generators as demonstrated by NASA's contribution to developmental research. Current deep space probes, as well as some satellites, have been powered by thermionic direct electrical converters in which electrons are "boiled off" between two materials with dissimilar work functions. While similar to TPV in some respects, this type of system is more mature but has little potential to exceed its present 10% operational efficiency (Angrist, 1988). If nuclear decay powered TPV converters at 20-25% efficiency could replace thermionic units, the power supply and endurance of such spacecraft would be greatly improved. NASA and other scientific interests have also examined TPV power sources for remote environmental sensing devices which currently use thermionics. Antarctic or ocean probes that monitor and transmit environmental conditions would have increased power and endurance with TPV systems.

In the maritime industry and the Navy, there is a useful niche for TPV power plants operating electric drive ships. Years of experience with electric drive ice breakers have proven that the electric propulsion alternative has several important advantages (Apriainen, 1993). The electric prime movers eliminate gearboxes and eliminate the need for any significant shafting, allowing much greater flexibility in ship design and stability. The power generators can be unitized and operated at peak efficiency outputs to match the total electrical load without limiting propulsion output, and the auxiliary power generators can be incorporated into these primary generators. This system allows for increased auxiliary power while reducing the total generating capacity, offers reduced noise and vibration, and includes high levels of reliability and redundancy. Current electric drive ships enjoy these benefits but suffer from increased weight, additional space requirements, increased fuel consumption and higher initial cost-- all of which can be reduced or eliminated by the inherent characteristics of a TPV power generator in place of diesel-electric sets (Belkhat, 1993). Short of taking over primary propulsion duties, TPV generators could offer many of the same advantages by replacing auxiliary power generators. Finally, the cogenerative arrangements previously mentioned find equal application to some marine propulsion systems to increase efficiency and reduce the need for dedicated auxiliary power capacity.

The operating characteristics of TPV systems offer a number of intriguing possibilities for military use. The Fort Monmouth Army Research Laboratory has been developing a portable power unit using a combustion fired TPV generator (Guazzoni, 1995). The system has potential application in large field generators for use in forward headquarters or medical units. Additionally, the Army has developed plans for a versatile covert power unit for use by special forces operating in hostile territory. This system is based on an array of photovoltaic cells which uses sunlight to power communications equipment or recharge battery operated devices during the day but can be reconfigured for TPV operation during darkness or adverse weather. The system is extremely light, compact and completely covert in either operating configuration.

The Navy has great potential to utilize the benefits of TPV technology. Naval surface units could operate electric drive ships with all of the advantages mentioned above, plus greater survivability due to the decentralized structure and the elimination of large engineering

compartments beneath the waterline. TPV cogeneration is particularly well suited to the gas turbine powered ships which exhaust a large portion of their developed thermal energy out of the stacks. A gas turbine could incorporate a TPV emitter and photovoltaic cells internally within the combustor, as shown in Figure 2-4 (Belkhat, 1993), or as an integral part of the turbine set. A simplified approach would be to simply use the high temperature exhaust to heat a separate TPV auxiliary power generator. Submarines could benefit from the low acoustic signature of TPV operation to reduce the cost of silencing machinery and minimize radiated noise. TPV power units could also be used for sonobuoys, decoys or any other high endurance deployable acoustic devices. Perhaps one of the most intriguing TPV applications, although completely undeveloped, is the use of TPV systems to cogenerate photons for laser pumping. Such optical pumps are required to provide the initial electron excitation to metastable states before lasing can occur, and utilize the type of narrowly tuned photon spectrum created by TPV generators. This laser output has uses in advanced communications, probing devices and laser weaponry (Belkhat, 1993).

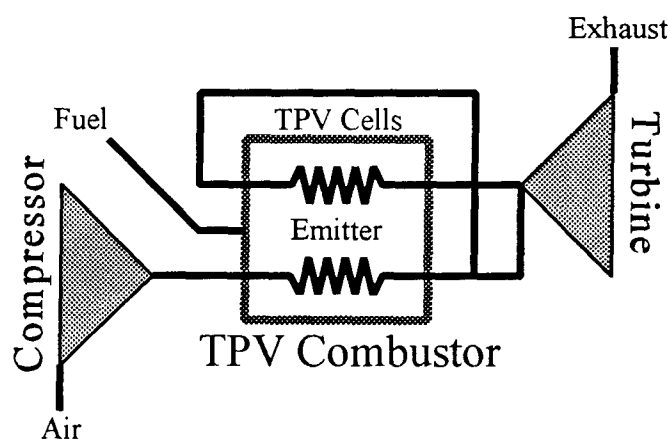


FIGURE 2-4: TPV Gas Turbine Cogeneration

3.0 PHASE I -- SUPPORTING RESEARCH

Achievement of the project objectives required summary study in a number of supporting engineering areas. The generation of energetic photons and their conversion to electrical power are the heart of the thermophotovoltaic concept and provided the baseline that all other processes had to support. The combustion phenomenon used for the thermophotovoltaic thermal source involved a number of interrelated parameters that had to be understood and controlled in order for an efficient high temperature flame to be developed. The system materials were critical to the success of the thermophotovoltaic photon generator as well, and they were carefully selected due to the demanding thermal engineering considerations. Sound understanding of each of these areas was necessary to generate photons at the target operational temperatures in a safe manner.

3.1 PHOTONIC PROCESSES

The TPV process can be divided into two distinct phases— photon emission and photon conversion. The photon emission phase encompasses the input of thermal energy into an emitter solid that releases the energy in the form of photon radiation. This radiation is characterized by its energy and wavelength as governed by a number of physical laws summarized in Table 3-1 (Kreith, 1993). The application of these equations provides the photon characteristics as a direct function of the emitter surface temperature and illustrates that there is a spectral curve of photon energies corresponding to any particular temperature as shown in Figure 3-1 on page 19 (Kreith, 1993).

TABLE 3-1: Physical Laws of Photon Emission

Photon Energy	$e_p = hv$	(3.1)
Stefan-Boltzmann Law	$E_b(T) = \epsilon \sigma T^4$	(3.2)
Wave Equation	$\lambda = \frac{c}{\nu}$	(3.3)
Wien's Displacement Law	$\lambda_{max} T = 2.898 \times 10^{-3}$	(3.4)
Planck's Law	$E_b(T) = \frac{C_1}{\lambda^5 (e^{C_2 / \lambda T} - 1)}$	(3.5)

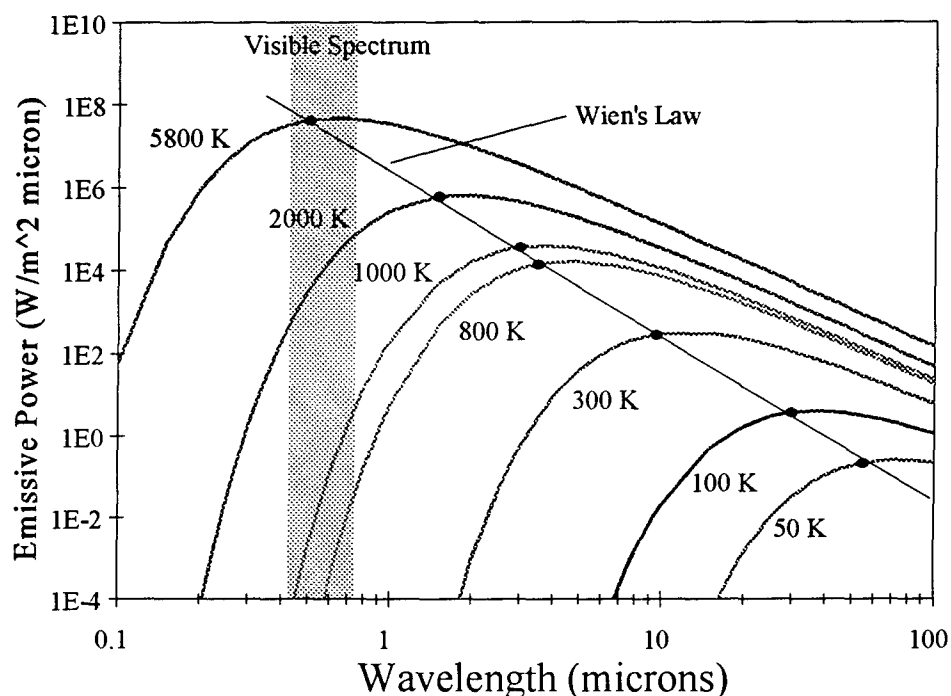


FIGURE 3-1: Blackbody Emissive Power

Specific materials have varying properties for converting input energy into emitted photons. This ability is a function of the material's absorptivity (α), reflectivity (ρ) and transmissivity (τ). In order to maintain the conservation of energy, any energy absorbed by a body must be radiated away as photons. A blackbody is a theoretical ideal emitter for which $\alpha=1$, meaning that all radiation incident to its surface is absorbed and subsequently emitted as photons. Real objects are called grey bodies because they reflect away a portion of the incident energy before it can be absorbed. The emissivity (ϵ) of a material is the ratio of the amount of energy that is actually absorbed and radiated as photons to the amount of energy that a blackbody would absorb and radiate. TPV system efficiency and power density are directly dependent on the efficiency of thermal to photonic energy conversion and therefore require a near blackbody emitter material.

The second half of the TPV process is the conversion of photons into an electrical current. This is accomplished within a semiconductor diode photovoltaic cell as illustrated in Figure 3-2 on page 20 (Angrist, 1988). Incident photon radiation undergoes a photoelectric reaction within the crystal structure of a semiconductor to generate an electron-hole pair which will develop a voltage differential across the depth of the diode. Due to the extremely high relaxation times of the photon-semiconductor reaction, six orders of magnitude faster than that for conduction processes, the electron-hole pairs can be generated

and utilized without heating the diode itself (Angrist, 1988). The extent to which incident photons are converted into electricity rather than heat within the diode determines the conversion efficiency of the cell. Current cells developed for TPV applications have shown 30% efficiencies (Duomarco, 1984), while 40% is believed to be achievable in the near future (Belkhat, 1993) and the theoretical limit approaches 85% (Chubb, 1993).

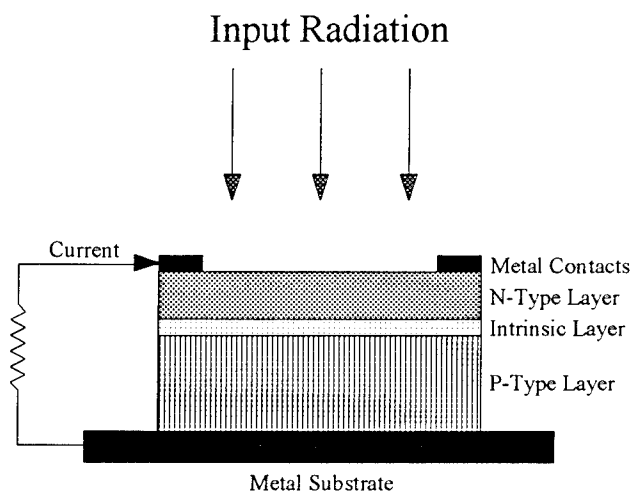


FIGURE 3-2: TPV Cell

The generation of an electron-hole pair in the semiconductor requires a discrete energy input called the band-gap energy. Depending on the material and structure of the photovoltaic cell, the band-gap energy varies from 0.25 eV to 3.00 eV (Chubb, 1992). If an incident photon's energy is less than the collecting cell band-gap, it cannot generate an electron-hole pair and the energy will be completely converted into heat. If the incident photon's energy is well above the cell band-gap, an electron-hole pair will be generated at its discrete energy level and the remaining energy will again be converted into waste heat. Therefore, efficient photon to electricity conversion requires that the photons striking the photovoltaic cells be tuned to a narrow energy spectrum corresponding to the band-gap energy of the specific cell type.

As previously discussed, the energy of the photons radiated from the emitter can be controlled by the emitter surface temperature, but only within the broad spectral ranges indicated in Figure 3-1. For a TPV system to be feasible, the photon radiation must be tuned to the photovoltaic cell band-gap in one of two ways. Some materials, called spectral emitters, do not follow the broad curves of a near blackbody and instead generate photons in very narrow energy peaks. If the emitter of the TPV system were constructed from such a material with an emittance peak corresponding to the band-gap of the photovoltaic cells,

conversion efficiency would be greatly improved. The second method is to place some type of spectral control filter between the blackbody emitter and the collection cells. Tandem plasma and interference filters have been developed which offer better than 90% reflection outside of a 1 micron window at the target band-gap. The non-band-gap photons are reflected back to the emitter where they are absorbed and re-radiated across the full energy spectrum. This is known as photon recycling and while it has the limitation of decreasing the output power density, it greatly increases the TPV conversion efficiency.

3.2 COMBUSTION

The first issue related to the combustion process is the selection of the optimal fuel. There are a wide range of available fuel gases, each with their own unique characteristics and advantages. As a comparative baseline, the Lower Heating Value (LHV) and adiabatic flame temperature of readily available gases were calculated and listed in Table 3-2 (McHenry, 1995). The complete calculations are included in the Appendix on page 61.

TABLE 3-2: Lower Heating Value and Flame Temperature of Fuels

FUEL	LHV (Btu/lb)	Flame Temperature (°F)		
		100% Oxygen	100% Air	400% Air
Hydrogen	51570	8711	4087	1446
Methane	21500	8918	3732	1252
Acetylene	20732	12860	4776	1542
Ethene	20277	10563	4161	1369
Ethane	20414	9372	3831	1273
Propene	19682	10281	4054	1333
Propane	19929	9526	3855	1277
Butane	19653	9604	3864	1277
Pentane	19497	9656	3871	1279
Benzene	17445	10972	4094	1326
Hexane	19390	9692	3876	1279
Heptane	19313	9717	3880	1281

The fuel Lower Heating Value represents the amount of heat that would be released if the products of combustion were to be cooled to standard temperature and pressure, assuming that the water products remain as vapor. This value indicates the maximum quantity

of heat that can be derived per unit mass of fuel reactant. From the table it can be seen that of the common fossil fuels, methane has the highest LHV of 21,500 Btu per pound of fuel. The table also shows the maximum theoretical flame temperature that each fuel can generate under various conditions. Combustion in pure oxygen produces the maximum temperature, while the presence of nitrogen in atmospheric air decreases this value. With a target emitter temperature of 2700°F, and allowing some margin for non-adiabatic combustion and heat transfer losses, all of the analyzed fuels had sufficient flame temperatures at the 100% air mixture. Due to these factors, as well as its common availability and low commercial costs, methane was selected as the combustion fuel source for the TPV photon generator.

Methane combustors can operate in one of six primary configurations depending on the level of reactant-oxidant mixing prior to combustion. Each of these configurations produces combustion and flame characteristics over a qualitative spectrum as illustrated in Figure 3-3 (Pocket Engineering Guide, 1971). While the majority of commercial combustors are type III or greater, the type I unmixed combustor configuration was selected. The engineering and construction requirements, as well as theoretical fluid modeling, are greatly simplified with separate air and gas entrances to the combustion chamber. Due to the high fuel preheat temperature above the ignition point predicted in the combustion system, the danger of explosive backfire was also minimized with the type I system. The excess flame temperature above the target for methane makes the type disadvantages of lower efficiency and longer combustion time acceptable.

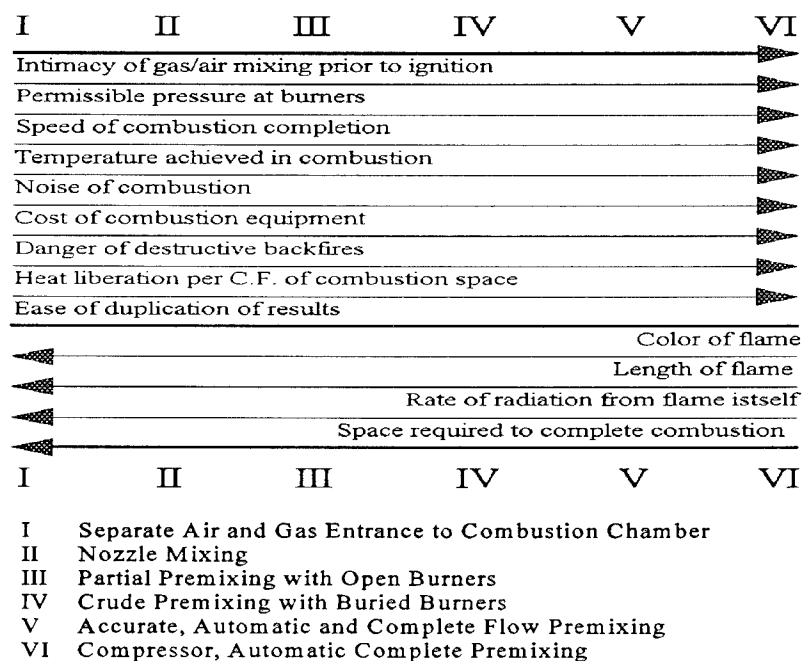


FIGURE 3-3: Characteristics of Combustor Types

3.3 MATERIALS

The demanding thermal engineering requirements on the combustor's components require that careful consideration be given to this issue. There are a number of important properties that will identify those materials which are suitable for TPV application. First and foremost is the material's melting point and softening temperature. The temperatures produced within the TPV combustion system exceed the melting points of all common metals and require that non-standard metals and various non-metal refractories be considered. The materials selected must also have excellent thermal shock resistance due to the rapid and extreme cycling that the burner will undergo as it is heated from room temperature to full operational temperature within a matter of seconds. The thermal conductivity of various system components must be considered as well. A highly conductive emitter material will optimize a uniform temperature distribution while the inlet and exhaust duct components should have low conductivities to minimize thermal losses from the system. When different materials are used together in close proximity the relative rates of thermal expansion must be compared to prevent destructive incompatibility. For the emitter surface, the material emissivity is a critical selection criteria to ensure that adequate efficiency and power density are achieved in the photon emission. Finally, the analysis of material properties must include pragmatic factors such as relative cost, machinability and safety in the high temperature combustion environment. To accommodate a preliminary comparative analysis, the pertinent characteristics of some possible materials are listed in Table 3-3 (Avallone, 1987 and Somiya, 1989).

TABLE 3-3: Material Characteristics

Material	Melting Point (°F)	Thermal Conductivity (Btu/hr ft °F)	Coefficient of Thermal Expansion (1/°F)	Emissivity	Availability	Machinability
Aluminum	1151	118	1.414×10^{-5}	.05	Good	Good
Copper	1917	223	9.120×10^{-6}	.02	Good	Good
Iron	2795	42.0	8.200×10^{-6}	.65	Good	Good
Steel	2765	25.0	7.200×10^{-6}	.06	Good	Fair
Tungsten	6034	94.0	2.470×10^{-6}	.39	Poor	Good
Pyrex	1508	.590	1.778×10^{-6}	.94	Fair	Poor
SiC- α	4028	70.0	2.500×10^{-6}	.96	Fair	Poor
Al ₂ O ₃ - α	3722	3.50	5.000×10^{-6}	.90	Fair	Fair
ZrO ₂	4919	1.17	5.000×10^{-6}	.95	Fair	Poor

The results of this preliminary materials search indicated that ceramic materials are required to operate in the target temperature regime due primarily to the insufficient melting points of the common metals. Ceramics refers to a wide variety of metallic and non-metallic compounds which form crystalline structures but have no free valence electrons. Ceramics can be further divided into the classical ceramics, which comprise familiar materials including brick, pottery and glass, and technical ceramics, which include modern electronic ceramics, structural ceramics and engineering ceramics. These materials, especially those in the technical family, are typically characterized by a number of thermal properties which make them ideal for such high temperature combustion applications as the TPV burner (Table 3-4; Somiya, 1989). From among this diverse group of ceramic materials, a number of primary candidates were apparent due to their outstanding thermal characteristics, emissive properties, and relatively wide availability.

TABLE 3-4: Typical Characteristics of Ceramics

High Melting Point
High Hardness
High Compressive Strength
High Shear Resistance
Brittleness
Low Electrical Conductivity
Low Thermal Conductivity
Low Thermal Expansion
High Corrosion Resistance

Alumina (Al_2O_3 - α) is the most common technical ceramic and has reached a mature stage of commercial development due to its relatively low cost and wide availability. The chemical composition Al_2O_3 refers to all alumina ceramics but the nature of the material varies widely with its crystalline form, the impurities present, and the particle size. It is the most stable of the oxide ceramics with excellent heat and corrosion resistance, and while the most common forms have limited useful temperatures, high purity aluminas have been used for applications approaching 3500°F. It has a broad emissive spectrum and a total emissivity value of 0.90 (Somiya, 1989).

Silicon carbide (SiC) is a ceramic material with a strong covalently bonded structure. It is the fastest growing of the modern industrial ceramics with hundreds of thousands of tons being produced around the world annually for use in steel-making additives, machining abrasives, refractory materials, and heating elements. It has two crystalline forms—the hexagonal or rhombohedral α phase and the cubic β phase. The β phase has poor properties and has found little application while the α phase exhibits good thermal stability, high heat

resistance, and outstanding corrosion resistance. Silicon carbide exhibits a near blackbody emissive spectrum with an emissivity value of 0.96 (Somiya, 1989).

Zirconia (ZrO_2) has seen remarkable development in recent years and is fast becoming a primary industrial ceramic. Basic zirconia ceramics undergo a crystalline phase shift near 2000°F which induces a large change in volume and resultant thermal shock fracture. To counter this, CaO , MgO , or Y_2O_3 is added which results in an isometric material called stabilized zirconia that will not undergo the phase shift. Even better material properties can be developed by using the internal stress of a dimorphous composition in partially stabilized zirconia. The result is a material with excellent compressive strength in addition to a useful temperature exceeding 4000°F , low conductivity and good emissivity properties (Somiya, 1989).

At the recommendation of Dr. Inna Talmy at the Naval Surface Warfare Center, White Oak Maryland, two alternatives to standard commercial ceramics were investigated. The Carborundum Company markets a line of Carbofrax silicon carbide mortars, and the Alcoa Corporation sells a similar calcium aluminate product marketed as CA-25. These phosphate based mortars are in the form of dry powders which undergo chemical bonding when mixed with water to form the ceramic compounds. These self mixed mortars offer an in-house method to fabricate simple geometries at a fraction of the time and cost of industrial ceramic procurement. Table 3-5 (Somiya, 1989) compares the properties of the primary candidate ceramics.

TABLE 3-5: Primary Ceramic Candidates

Material	Hardness (Rockwell A)	Compressive Strength (psi)	Melting Point ($^\circ\text{F}$)	Thermal Conductivity (Btu/hr ft $^\circ\text{F}$)	Coefficient of Thermal Expansion ($1/^\circ\text{F}$)
$\text{Al}_2\text{O}_3\text{-}\alpha$	95	10000	3722	3.5	5.00×10^{-6}
$\text{SiC-}\alpha$	97	115000	4028	70	2.50×10^{-6}
ZrO_2	91	90000	4919	1	5.00×10^{-6}
Carbofrax 8P	≈ 96	unknown	2900	≈ 70	unknown
Alcoa CA-25	unknown	≈ 30000	3200	unknown	unknown

From this data, and limited high temperature experimentation, the final materials for the photon emitter were selected. The two mortar alternatives were favored due to their significant cost and procurement time advantages, although the Carbofrax 8P suffered severe oxidation corrosion below 2700°F and was therefore eliminated from further consideration.

The Alcoa CA-25 demonstrated excellent high temperature stability and corrosion resistance, and was subsequently alloyed with pure alpha silicon carbide powder to optimize its blackbody emissive character. The conventional ceramics were also pursued in parallel to provide a comparison to industry standard products and to provide backup alternatives if the CA-25 mortar was not satisfactory. The final design included three emitter cylinders made from silicon carbide, zirconia, and CA-25 mortar, while the balance of the combustion system was made from the alumina alone.

4.0 PHASE II: SYSTEM MODELING

Application of the Phase I research began by defining the TPV photon emitter system. This was done by relating the controlling mathematical relationships for the combustor's fluid flow, combustion reaction and heat transfer. The resulting complex system of interrelated equations was solved using an iterative spreadsheet simulation. This computer model of the TPV burner was an invaluable design tool for the optimization of system performance and, after empirical validation, allowed for testing of various geometries and materials without the need for actual construction.

4.1 MATHEMATICAL RELATIONSHIPS

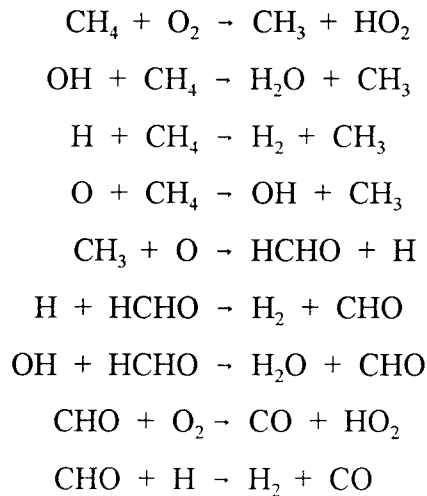
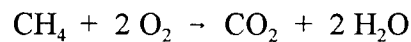
The fluid flow within the burner consisted of the gaseous methane fuel and the compressed air traveling through tubing and entering the combustion chamber. The basic flow properties that were determined included pressure, velocity, Reynold's number, head loss, density, and viscosity. Values such as pressure and velocity were calculated for their own merit as key factors in the overall design while the others were secondary values for the calculation of other properties. Table 4-1 lists the basic equations used (Lindeburg, 1992).

TABLE 4-1: Fluid Flow Equations

Pressure Drop	$\Delta P = h_f \times \rho \left(\frac{g}{g_c} \right)$	(4.1)
Velocity	$V = \frac{\dot{m}}{\rho A}$	(4.2)
Reynolds Number	$Re = \frac{\rho V D}{g_c \mu}$	(4.3)
Head Loss	$h_f = \frac{F L V^2}{2 D g_c}$	(4.4)
Density	$\rho = \frac{P}{R T}$	(4.5)

Gaseous combustion phenomena are not precisely understood and the analysis of the combustion process can become quite complex. In its most fundamental form, combustion is a simple chemical oxidation reaction. The basic chemical equation for the oxidation of methane is given in the upper half of Table 4-2. Actual high temperature methane combustion reactions, while centered on the basic equation, involve the formation and interaction of several intermediate species listed in the bottom half of Table 4-2 (Bernard, 1985). The exact role of each reaction is dependent on a variety of factors such as the reaction temperature, pressure, and the chemical composition of the encompassing solid. The impact of these secondary reactions on the flame performance can be significant for premixed flames, but they are much less critical in unmixed diffusion flame combustion due to the nature of the reaction zone. For this reason, simplification of the analysis by assuming that the combustion reaction will follow the basic oxidation equation was justified.

TABLE 4-2: Methane Combustion Reactions



In order to quantify the flame's role in heating the emitter surface, the heat output and flame temperature were required. The amount of heat a fuel generated in combustion was characterized by a number called the heating value— either Higher Heating Value (HHV) or Lower Heating Value (LHV), depending on the disposition of the water products of the reaction. The water products of the designed TPV burner remained in vapor form and therefore the LHV of the fuel was applicable. It was calculated as the difference between the

heat of formation of the reactants and the heat of formation of the products. Dividing by the molar mass of methane, the heat output per mass of fuel burned was determined. The total thermal power output was the product of this value times the mass flow rate of the methane. Actual combustors will not completely burn all available fuel and the combustion efficiency must be factored into the final value. Complete calculations are listed in the Appendix on page 61.

The energy liberated during combustion was used to heat the reaction products to the ultimate flame temperature. The enthalpy of the products as a function of temperature, in conjunction with the chemical equation, was used to calculate the temperature reached by the liberation of the LHV heat. For the TPV application, the combustion occurred in atmospheric air which could be accurately approximated as 3.76 moles of nitrogen (N_2) per mole of oxygen (O_2). Including the enthalpy of the nitrogen carried through the combustion heating process reduced the resultant flame temperature relative to pure oxygen combustion. By increasing the amount of excess air in the combustion zone, the mass fraction of inert nitrogen which had to be heated with the combustion products was increased, resulting in a lower flame temperature. Varying the air-to-fuel ratio, the amount of cooling air was controlled and thus the combustion reaction was manipulated to produce the target temperature of the emitter for the efficient generation of TPV photons.

The primary calculations defined in the TPV system were the heat transfer equations. Each of the three modes of heat transfer (conduction, convection and radiation) played important roles in the analysis. The combustion products were generated at the flame temperature and convectively and radiatively heated both the inner surface of the emitter body and the flame tube itself as illustrated at region (1) of Figure 4-1 on page 30 (McHenry, 1995). The flame tube reached an equilibrium by transferring that heat to the unburned fuel within it by convection, down its length to the supporting structure by conduction (2), and to the inner surface of the emitter body by radiation (3). The emitter body received heat through the combustion product convection and flame tube radiation, and transferred it primarily to the photovoltaic cells by radiation, although some conduction to the supporting structure and surface cooling convection occurred (4). The photovoltaic cells converted the majority of the incident thermal radiation into electricity while cooling water removed waste heat (5). The losses to the system included all conduction down the length of the emitter and flame tube into the supporting structure, the convective cooling in free air of the emitter surface, and the large amount of heat carried out of the combustion chamber by the hot exhaust gases.

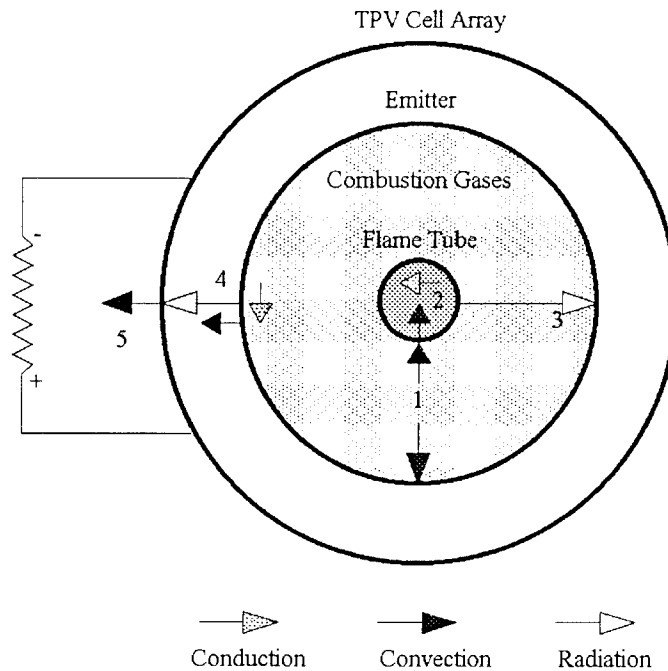


FIGURE 4-1: Combustor Heat Balance

Calculations of the heat transfer was straightforward and applicable equations are listed in Table 4-3 on page 31 (Kreith, 1993). Conduction was defined by Equation 4-6 and required only the total heat flow (Q), the temperature differential across the conductive transfer distance (dT/dx), and the thermal conductivity of the material (k). Equation 4-7 governed convective heat transfer and required the same heat and temperature numbers along with the convection coefficient (h_c) which was determined from a number of empirical formulas depending on the fluid flow conditions and the transfer geometry. While both conduction and convection were important in the system heat balance, radiative transfer is a function of the material temperature to the fourth power and dominated in the burner at the high operational temperatures. Equation 4-8 defined the radiative transfer rate as a function of the shape factor (F), material emissivity (ϵ), Stefan-Boltzmann constant (σ), and the emission temperature (T).

TABLE 4-3: Basic Heat Transfer Equations

Conduction	$Q_k = kA \frac{dT}{dx}$	(4.6)
------------	--------------------------	-------

Convection	$Q_c = h_c A \Delta T$	(4.7)
------------	------------------------	-------

Radiation	$Q_r = F \epsilon \sigma T^4$	(4.8)
-----------	-------------------------------	-------

4.2 COMPUTER MODELING

While each of the governing system properties was based on a relatively simple equation, due to the interdependence of the variables the solution of the complete system was beyond manual calculation. A Quattro Pro® for Windows spreadsheet was programmed by Associate Professor Keith W. Lindler of the U.S. Naval Academy Naval Architecture, Ocean and Marine Engineering Department (Lindler, 1995) to model the fluid flow, combustion reaction and heat transfer of the TPV system and to solve for the critical design parameters. It was a versatile computer simulation that allowed the user to input the physical geometry and combustion reactant flow properties and obtain all critical values for fluid flow, chemical combustion, and heat transfer. The computer model considered the TPV combustor as 20 mathematical nodes for analysis, calculating the values of the system properties within each node and the influence of those values on adjacent nodes. The model consisted of a number of consecutive notebook "pages" in the Quattro Pro® file, with each page displaying a system property calculated using the properties on other relevant pages. Table 4-4 on page 32 is a page listing for the computer program (Lindler, 1995).

TABLE 4-4: Computer Model "Pages"

Page 1	CONTENTS	Button driven program contents
Page 2	DATA INPUT	User defines system constraints
Page 3	PRESSURE	Calculates fluid pressures
Page 4	VELOCITY	Calculates fluid velocities
Page 5	REYNOLDS NUMBER	Calculates flow Reynolds number
Page 6	HEAD LOSS	Calculates flow head loss
Page 7	TEMPERATURE	Calculates system temperatures
Page 8	DENSITY	Calculates fluid densities
Page 9	VISCOSITY	Calculates fluid viscosities
Page 10	MASS FLOW RATE	Calculates fluid mass flow rates
Page 11	CONVECTION COEF.	Calculates heat transfer coefficient
Page 12	CONVECTION TRANSFER	Calculates convective heat transfer
Page 13	RADIATION TRANSFER	Calculates radiation heat transfer
Page 14	CONDUCTION TRANSFER	Calculates conduction heat transfer
Page 15	PRESSURE DROPS	Calculates flow pressure drops
Page 16	NET ENERGY TRANSFER	Calculates total heat transfer
Page 17	MATERIAL PROPERTIES	User inputs material properties
Page 18	FUEL PROPERTIES	User inputs fuel properties
Page 19	OXIDANT PROPERTIES	User inputs oxidant properties
Pages 20-23	GRAPHS	Displays of temperature output
Pages 24-29	HELP	Explanative text pages

The TPV computer model solution was driven by the data input page, show as Figure 4-2 on page 33 (Lindler, 1995), where the user defined the system. On the computer screen, color coded values were variable inputs or numbers either calculated or tabulated by the program. The materials for each component were entered and the corresponding material properties were automatically retrieved from the "Material Properties" page. The geometrical attributes, which were input, included the diameters and lengths of each cylindrical component. The precise configuration of the flame tube was controlled by programming the number and size of holes for gas flow within each of the 20 nodes. The heating of the burner was controlled by the fuel inlet pressure which governed the fuel mass flow rate, while the program calculated the oxidant flow requirements to maintain the input air-to-fuel ratio. The section at the upper right allowed for the definition of a heat exchanger to recuperate some of the exhaust heat and modeled the combustion efficiency and burn time. Finally, the values in the bottom right hand corner of the screen were the user input weighting factors used to assure that the complex system of equations remained stable and converged to a solution.

2

Context:

Data Input

Flame Tube					
Material	Steel	p	487	thick	0.05 in
I.D.	0.800 in	c	0.113	Area i	1.89845 in ²
O.D.	1.000 in	k	25	Area o	1.884856 in ²
Length	12 in	c	0.35	Area x	0.149228 in ²
Len/seg	0.6 in	a	7.2E-08	mass	0.025224 lbm

Emitter					
Material	Steel	p	487	thick	0.0025 in
I.D.	3.250 in	c	0.113	Area i	6.128108 in ²
O.D.	3.375 in	k	25	Area o	6.361725 in ²
Length	12 in	c	0.35	Area x	0.050408 in ²
Len/seg	0.6 in	a	7.2E-08	mass	0.109982 lbm

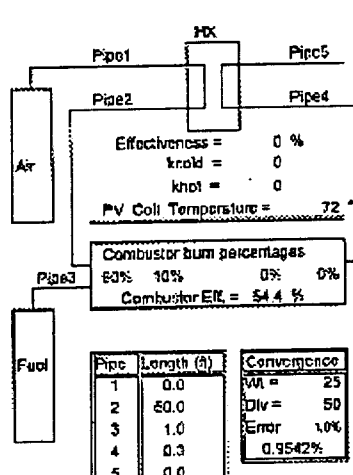
Connecting Pipes					
Material	Copper	p	559	thick	0.031 in
I.D.	0.638 in	c	0.0915	Area i	25.93598 in ²
O.D.	0.750 in	k	223	Area o	20.27433 in ²
Length	chart	c	0.023	Area x	0.070023 in ²
		a	9.1E-08	mass	0.271825 lbm

	Type	Pressure (psia)	Temperature °F
Fuel	Methane	14.960	30
Oxidant	Air	18.068	30
Ambient		14.700	72

Fuel flow rate (calculated)	3.3081 lb/hr	
Fuel flow (experimental)	3.1103 lb/hr	
Air/Fuel Ratio (lb/lb)	13.941	-0.08 excess oxygen (lb/lb air)

Flame Tube		
	Number of holes	Hole Diameter (in)
1	18	0.0210
2	4	0.0210
3	4	0.0210
4	4	0.0210
5	4	0.0210
6	4	0.0210
7	4	0.0210
8	4	0.0210
9	4	0.0210
10	4	0.0210
11	4	0.0210
12	4	0.0210
13	4	0.0210
14	4	0.0210
15	4	0.0210
16	4	0.0210
17	4	0.0210
18	4	0.0210
19	4	0.0210
20	4	0.0210

PV dia	99.030
PV emiss	0.99



Pipe	Length (ft)	Conductance
1	0.0	W = 25
2	50.0	Div = 50
3	1.0	Error 1.0%
4	0.3	0.9542%
5	0.0	

Fuel LHV	21504	Btu/lb
Fuel R	88.32	R-Btu/lbm°R
Fuel k	1.209	1.3
Oxidant R	53.65	R-Btu/lbm°R
Fuel Cp	0.538	Btu/lbm°R

FIGURE 4-2: Data Input Page

Using the information provided on the "Data Input" page and derivatives of the relationships outlined in Section 4.1, the spreadsheet proceeded to solve the system of simultaneous equations. Each subsequent page was laid out to graphically represent a schematic of the TPV system, displaying the calculated values in the correct position. The "Radiation Heat Transfer Rate" page is included as Figure 4-3 to illustrate a typical page layout. The methane fuel entered from the bottom left as shown and flowed through holes drilled in the flame tube where it reacted with the air and generated high temperature combustion gases. These gases exited the combustion chamber to the right and passed through the heat exchanger before exhausting to the atmosphere. The numbers displayed along the length of the combustor were the radiative heat transfer rates for each particular component at that mathematical node. The model calculated the radiative transfer from the flame tube to the inner surface of the emitter and from the outer surface of the emitter to the TPV cells. In order to calculate the radiative heat transfer, the model linked the equations on this page to the geometric data from the "Data Input" page, the component temperatures from the "Temperature" page, and the heat flow in the emitter from the "Convection Heat Transfer Rate" and "Conduction Heat Transfer Rate" pages. It should be noted that the "Temperature" page was dependent on this radiative heat transfer calculation and that the other heat transfer pages were dependent on those temperature values. It was this complex interdependence of the system properties that required reliance on iterative computer simulation.

Contents

Radiation Heat Transfer Rates (Btu/hr)

13

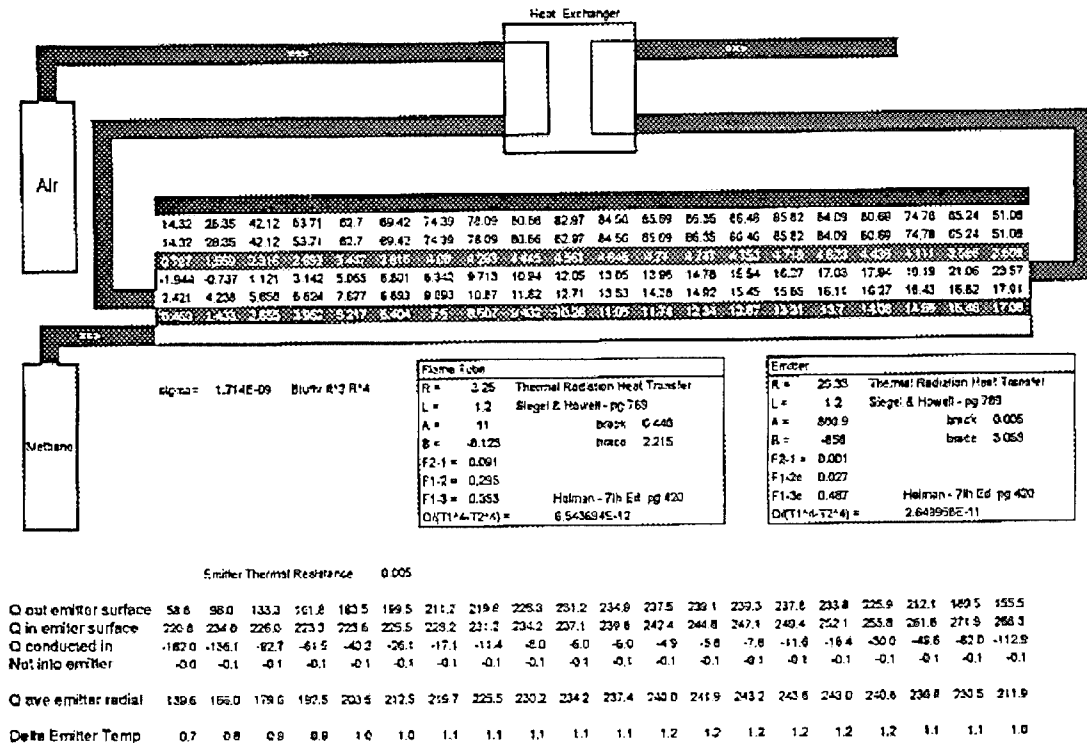


FIGURE 4-3: Radiation Heat Transfer Page

In order to validate the model, two types of verification were conducted. First, an independent manual calculation of all output values was performed. To complete this manual calculation, the node number ten pressure equation was arbitrarily selected as an initial point. The pressure values were determined by the pressure change from the known atmospheric exhaust pressure, and the values of the pressure change were a function of the density, velocity and head loss calculations. Each of these values is dependent on another branch of calculations, and the verification process was continued. Eventually each of the properties were calculated and compared to the computer solution, showing full agreement. This process eliminated the chance of internal mathematical errors within the program.

The second source of validation was the empirical comparison conducted during Phase III prototype testing. Experimental data was taken from a test plan covering a wide range of flow conditions and geometries. As this data was plotted against computer predicted curves, the major sources of error were identified and corrected. Over the course of the project the TPV computer model evolved through over 150 versions as additional calculations and corrections were programmed. Program version 66 characterized the early model versions, greatly over-predicting component temperatures and containing anomalies such as

fluid flow against a pressure gradient and exhaust gas temperatures exceeding the maximum adiabatic flame temperature of combustion. These anomalies were the result of incomplete modeling, system instability, and internal errors. The turning point for the model results occurred with TPV version 92. This version had evolved to include the calculation of fluid viscosity as a function of temperature, complete Reynold's number calculations, and combustion efficiency considerations among other improvements. Version 92 exhibited drastically improved convergence and system stability, and eliminated the output of obvious physical impossibilities although it still tended to over predict final temperatures. The final TPV model built on version 92 by calculating the convection heat transfer coefficients, accounting for all conductive and convective thermal losses, and allowing more control over the efficiency of the combustion process. It was free from any sign of system instability and converged rapidly to accurate predictions. Figure 4-4 (McHenry, 1995) provides a comparison of the temperature predictions of the three model versions discussed above, converged to the same combustor configuration.

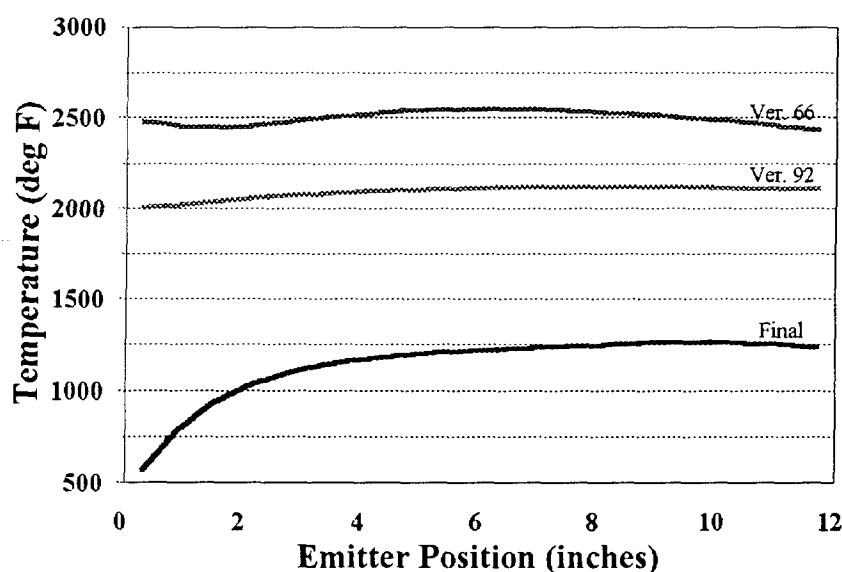


FIGURE 4-4: Evolutionary Model Development

The mathematically and empirically verified computer model was the primary tool for the optimization of the final U.S. Naval Academy TPV photon emitter design. It was used to indicate the required reactant flow rates needed to achieve target temperatures, the amount of recuperation necessary and the resulting thermal efficiency, the effect that different emitter materials had on system performance, and all other design consideration which had to be addressed.

5.0 PHASE III: PROTOTYPING

The early versions of the TPV computer program were used to generate an initial prototype design. This prototype was built from materials readily available within the U.S. Naval Academy Engineering and Weapons Division machine shop and was operated at approximately half of the ultimate target temperature. The effort to design, build and operate the prototype TPV combustor proved to be extremely valuable and accomplished the stated objectives of gaining operational experience while validating the computer model.

5.1 DESIGN

The design of the prototype burner incorporated three competing needs. First, the value of the prototyping process was maximized by close correlation between the test burner and the expected final design. The general size, shape and operation of the final apparatus were constrained by the DOE agreement and these constraints were incorporated into the prototype as much as possible. The second requirement was that the prototype be as simple as possible. This was necessary for fabrication and construction as well as for the ability to model the system characteristics accurately within the TPV computer program. Finally, the system had to be designed in such a way that accurate measurement of integral values could be taken and recorded reliably.

The first design priority was the consideration of available materials. The Engineering and Weapons Division machine shop regularly works with all common metals including copper, aluminum, iron, and steels which they can silver solder, braze or weld. Pyrex glass cylinders were also available in a limited range of sizes. The use of Pyrex for the emitter cylinder allowed for visual inspection of the combustion process which enabled ignition methods to be verified and the flame character to be well represented within the computer model. It also allowed the temperature of the internal flame tube to be monitored based on its radiative color. The Pyrex could withstand temperatures up to 50% of the ultimate target emitter temperature and had a high emissivity value ($\epsilon = 0.96$). For these reasons, the largest Pyrex cylinder in stock, with a 3.35 inch diameter, was used to establish the combustion chamber size. Its softening point of 1500°F limited the maximum operating temperature. Based on this 1500°F emitter temperature, the predicted flame tube temperature was approximately 2200°F and the exhaust duct temperature was 1800°F. These values required the use of type 304 stainless steel for the flame tube while mild steel and copper were used for the remaining components.

With the materials selected, the prototype system was designed to fulfill the DOE requirements while allowing for accurate modeling and enabling data measurement. The resulting burner was 12 inches long and composed of a 1.00 inch outer diameter (OD) type 304 stainless steel flame tube inserted coaxially into a 3.35 inch OD Pyrex glass emitter tube. A mild steel air header accepted inlet air and distributed it to four air legs entering the combustion chamber and radially surrounding the flame tube. The flame tube was threaded through the base plate of the combustion chamber and screwed into a 0.75 inch copper fuel inlet line. At the upper end, a mild steel top plate sealed the chamber and channeled exhaust gases into the 1.50 inch OD steel exhaust duct. The flame and emitter tubes were designed in such a way as to make them easily interchangeable and included the necessary thermal engineering requirements. The emitter tube was seated in a 0.25 inch deep groove milled out of both the top and base plates and was held in place by eight set screws. The flame tube could be unscrewed and removed completely from the base plate and it was not connected to any other portion of the combustion chamber. This design allowed for the Pyrex emitter tube and stainless steel flame tube to freely expand in the vertical direction at the radically different rates dictated by their coefficients of thermal expansion. Figure 5-1 on page 38 is a sketch of the combustion chamber while engineering drawings of the individual components machined in the U.S. Naval Academy shop are included in the Appendix on pages 66-70 (McHenry, 1995).

Intuitive design, in conjunction with the predictions of a primitive version of the TPV computer model, was used to determine the configuration of the flame tube holes. With the need to develop a linear temperature profile along the emitter length and the fact that the inlet air temperature was 1400°F cooler than the target temperature, it was foreseen that there would be a steep temperature gradient in the lower portion of the apparatus as the air was heated in combustion and the resultant gases transferred heat to the emitter. In order to minimize this temperature gradient, a large percentage of the gas had to be burned near the air inlet to increase the temperature as rapidly as possible while combustion was maintained down the length of the flame tube to prevent a fall-off in temperature. The computer model was used to optimize a design, resulting in a prediction that less than 5% variation in temperature could be achieved for the upper 9 inches of the emitter surface. The resulting design called for sixteen 0.06 inch diameter holes to be drilled radially 0.30 inches from the air inlet with a series of four 0.01 inch diameter holes drilled radially every 0.60 inches up the remainder of the flame tube.

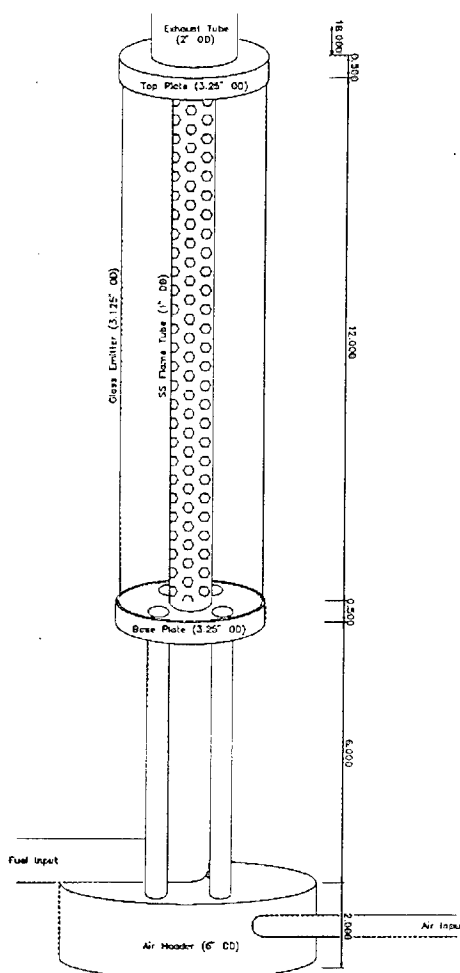


FIGURE 5-1: Prototype Design

The complete experimental system included the air and fuel sources, exhaust ducting, and measurement equipment. The air source consisted of a 500 ft³ air bank running through a six lead whip into a high pressure needle valve used to control the air flow. From the valve, the air line ran through a variable area rotameter to measure the flow rate, past a pressure gauge, and into the air header. The fuel source was a 384 ft³ methane cylinder tapped with a pressure regulator. From the regulator, the fuel line ran through a second rotameter, past a pressure gauge, and through an emergency cut-off ball valve before entering the flame tube inlet. The high temperature exhaust gases exited the exhaust tube into a specially constructed 4 ft² stainless steel hood hanging from a 3.00 inch exhaust duct connected to an external test cell fan. This design used the venturi effect to entrain cool atmospheric air into the exhaust

stream, eliminating the need for any extensive exhaust handling mechanism. Temperature measurements were taken with an array of 16 type K thermocouples connected through an analog to digital converter to a personal computer. The computer was used to log temperature data across the 16 channels every 2 seconds for the duration of each test run. The thermocouples measured the emitter temperature profile as well as the temperatures of the steel supporting structure to determine conduction losses and the temperature of the exhaust gas stream to monitor combustion performance. A schematic of the entire system is shown in Figure 5-2 (McHenry, 1995).

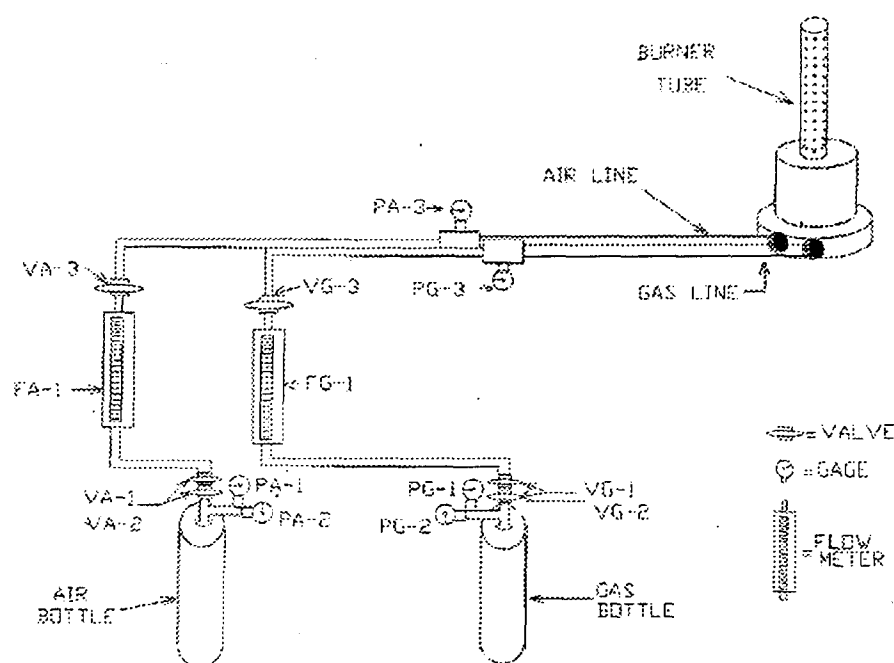


FIGURE 5-2: Complete System Schematic

5.2 SYSTEM CONSTRUCTION

The complete TPV photon emitter prototype was constructed from existing materials in the Engineering and Weapons Division machine shop and laboratories within the Rickover Hall complex at the U.S. Naval Academy. All of the tubing, including the Pyrex emitter, stainless steel flame tube and inlet and exhaust ducting were available from existing stock supplies. The mild steel air header and combustion chamber end plates were machined to specs out of steel block. All joints were completely welded and checked for air tightness with the exception of the copper inlet lines which were silver soldered into the steel structure.

The only difficulty in construction arose from the design configuration of holes along the length of the flame tube. The conventional high speed drill presses on site could not be made to drill the 0.01 inch diameter holes in the extremely hard stainless steel tube. Due to the small hole size, a center tap could not be used and the drill bits walked along the curvature of the tubing instead of biting into the metal. The computer model was consulted and it was determined that the initial hole size dominated the flow and that the downstream holes could be doubled in size without drastically changing the predicted temperature profile. High strength 0.021 inch carbide drill bits were ordered and used successfully to drill the series of 76 holes without further difficulty. The size of the first set of 16 holes was also adjusted to a 0.062 inch diameter to conform to standard drill bit sizes.

The remainder of the prototype system, consisting of high temperature hose for the inlet gases, pressure gauges, valves, hose fittings, thermocouples and computer equipment, was assembled from existing laboratory supply. The entire apparatus was built on a mobile test bench within an explosion proof engine testing cell. Figure 5-3 on page 41 is a photograph of the U.S. Naval Academy prototype TPV combustor (McHenry, 1995).

5.3 PROTOTYPE OPERATION

The prototype TPV system was designed to be both easy and safe to operate. A detailed step-by-step operating procedure was developed and used in the experimentation and is included in the Appendix on pages 72-73. The initial steps ensured the safety of the operator and uninvolved personnel by clearing the immediate area, providing safety equipment and securing the test cell doors. Once the area was safe for combustion, a series of pre-ignition steps were taken. First, the thermocouple contacts were verified and the computer was configured to log the data correctly. The fuel and air lines were then charged and the emergency cut-off valves were opened. To initiate combustion, a slight air flow was established followed by the introduction of the methane. A piezoelectric crystal in a simple push-button device was then used to generate a spark from a modified thermocouple wire to the flame tube. Once a flame was established, the flow rates were adjusted slowly to the operational targets. All temperature data was logged automatically, while a hand held calculator was programmed to convert the flowmeter readings and the operator recorded the pressures directly.

As intended, the construction and operation of this prototype burner generated several important lessons learned that would be critical for the final apparatus design. The first issue concerning ignition was foreseen but underestimated. Due to the low conductivity of the methane gas itself, it sometimes took several discharges from the piezoelectric crystal before a flame occurred. During this time, the methane gas was filling the combustion chamber, the exhaust tube, and the exhaust ducting. When ignition finally did occur there was the potential for an explosion. The system was designed with enough free exhaust area to prevent such an explosion from being overly dangerous or destructive, but this situation had to be avoided.

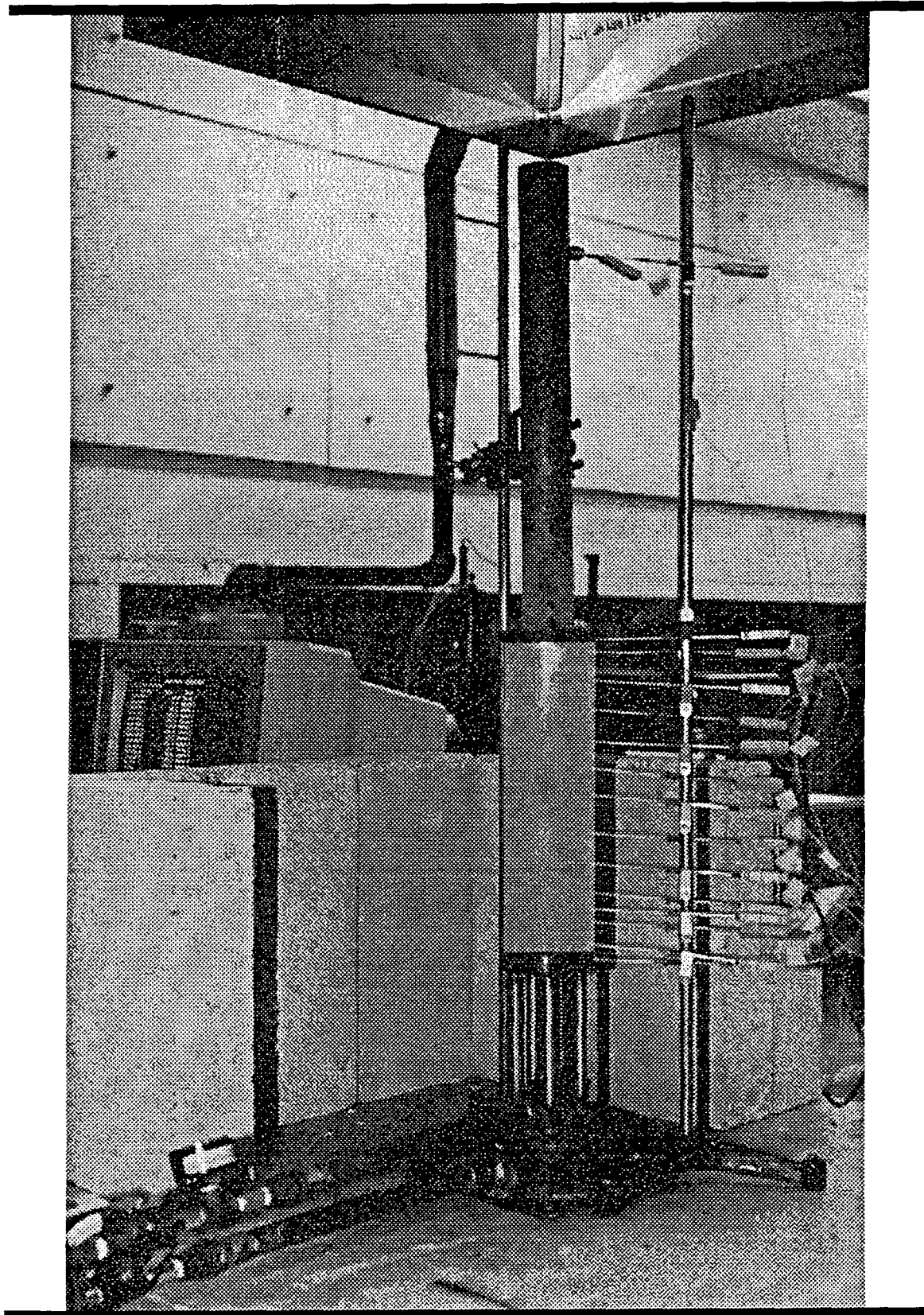


FIGURE 5-3: TPV Burner Prototype

Operational experience led to the determination of the minimum gas flow rate at which ignition could occur and this very low flow was used for all ignitions to minimize the methane build-up within the system. If the spark failed to ignite the gas after three quick consecutive discharges, the gas flow was shut off so that the air flow could clear the combustion chamber and exhaust ducting.

The second issue involving ignition was the effect that the spark ignitor had on the personal computer. The piezoelectric crystal generated almost no current but it did generate a significant voltage. When this voltage was discharged to the metallic structure of the TPV burner, the only ground path provided was the thermocouple wire touching the metal surface and leading back to the computer. Although the thermocouples were separately grounded, the resulting electrical shock caused software malfunction and eventually burned out the chips on the data acquisition card. To remedy the situation two steps were taken. The computer was configured prior to ignition and then powered down. This allowed the voltage to be dissipated through the thermocouple grounding circuit without damaging the computer components. Once ignition occurred, the computer was rebooted and data logging began. A second step taken was to provide an alternate ground path from the burner structure itself. This was accomplished with a ground wire being clipped onto the air inlet duct, or more often, simply having the operator touch the inlet piping as he depressed the push-button ignitor.

The third valuable lesson learned concerned the flame stability within the combustion chamber, and was positive reinforcement of the value of the Pyrex emitter tube. As flow rates were increased, the flame front could be seen to rise up the height of the flame tube until eventual complete blowout occurred. This was an indication that the flow velocity was exceeding the flame velocity of the combustion, although the manual and computer calculations did not indicate flow velocities in that range. The answer was that the theoretical calculations did not accurately model the physical device. Where velocity calculations used the 5.25 inch² flow area between the flame tube and emitter, the actual air inlet consisted of four air legs with a total area of only 0.50 inch². This difference increased the actual air velocity by a factor of 12 over the calculated value, forming high speed air jets which could not support combustion. To solve the problem, a simple air diffuser plate was designed and manufactured. Inserted between the four air inlets and the combustion zone, this plate simply blocked the high speed jets and functionally increased the inlet flow area to allow the flow velocity to reach the calculated values. When put into operation it was discovered that not only did the diffuser fulfill its purpose in slowing the velocity, it also acted as a static flame holder forming the base of the combustion zone and greatly increasing the system stability. As higher flow rates and temperatures were reached, the flame became unstable and began to oscillate noisily. Study of the combustion process in operation indicated that this time the flame front remained intact on the diffuser plate, eliminating excess flow velocity as the cause. Instead, it was discovered that the thermal expansion of the diffuser plate loosened its connection to the flame tube and allowed it to vibrate in the higher velocity air flows. This vibration set up shock waves in the combustion gases which caused the unstable combustion

that was observed. The problem was rectified by modifying the diffuser plate connection to include a simple expansion wedge that eliminated the vibration.

While the Pyrex emitter did prove its worth in the identification of problems within the combustion reaction, it was soon determined that it was not suitable for continued use. The first problem was the common brittleness of glass. Subjected to even the unavoidable stresses of transport and handling, the glass cylinders chipped and shattered repeatedly. This problem was partially solved by annealing the cylinders prior to use, but the strength was still only marginally acceptable. The surface of the glass was also very smooth and the inability to exert pressure on the cylinder limited the ability to maintain adequate thermocouple contact. During the vibration of ignition, several of the thermocouples would slip off of the face of the glass and cease to log accurate data. To counter this, two steps were taken. First, the area of contact was sand-blasted to roughen the surface and prevent slippage. Second, the thermocouple array was configured such that two complete temperature profiles were measured in parallel. This provided a backup probe at each location so that one complete profile could be generated, but it also halved the density of measurements. Finally, the Pyrex proved unable to withstand the high temperature conditions. It had marginal thermal shock resistance and would often crack following ignition if the temperature was increased too rapidly. The result was greatly extended experimental runs with only a limited time at steady state temperature. Although the softening point of Pyrex is published as 1508°F, under the internal pressure of the air flow and the external point pressure of the thermocouples, catastrophic deformation began near 1000°F. Aggravating this problem was the danger of the glass emitter tube failing under pressure and incurring shrapnel injury, thus requiring extensive shielding for the operating personnel. All of these issues taken together made the completion of the prototype operation goals impossible with a glass emitter tube.

Following completion of the fluid flow and combustion process observations, the glass tube was replaced by a stainless steel emitter tube. This change effectively eliminated all of the problems listed above and produced trouble free operation. With the sturdy steel emitter in place, the pressure of the thermocouple contacts could be increased to improve temperature accuracy. To facilitate reliable contact, the thermocouple probes were spring loaded so that constant pressure would be maintained and they could follow vibrations caused by ignition. With these improvements made, the thermocouples suffered only a 5% failure rate and the parallel arrays were eliminated to increase profile resolution. In this final configuration, the computer data acquisition system recorded temperatures at 12 points along the length of the emitter in addition to the base plate and top plate temperatures and the exhaust stream and exhaust duct temperatures.

5.4 EXPERIMENTATION

Once the operational procedures had been established and the combustor was modified to produce steady and repeatable performance, the experimental data collection process began. The goal of the experimentation plan was to record steady state temperature

data under a number of different flow conditions in order to test and calibrate the TPV computer model's prediction ability. Although the glass emitter was replaced early in the experimentation plan, data taken from those initial runs also provided the opportunity to test the model with varying materials.

The computer data acquisition system logged the temperature data for each of the 16 thermocouples, along with a time stamp, every 2 seconds. This file was saved to the hard disk as a comma delimited text file which was displayed as a lengthy string of numbers. In order to reduce the data into meaningful temperature profile curves, the files were imported into the Quattro Pro® for Windows program where they could be manipulated and plotted. The first step was to organize the numbers into a 17-column array where each row represented one time step of data. The array was labeled with the appropriate pressure and flow values which defined each experimental run. The time stamp was then converted into decimal form and normalized to produce a simple run time value in seconds. This time dependent data was plotted to illustrate the experimental run dynamics and to define steady state regions for further analysis. Figure 5-4 is a plot of the exhaust gas temperature during a typical experimental run (McHenry, 1995).

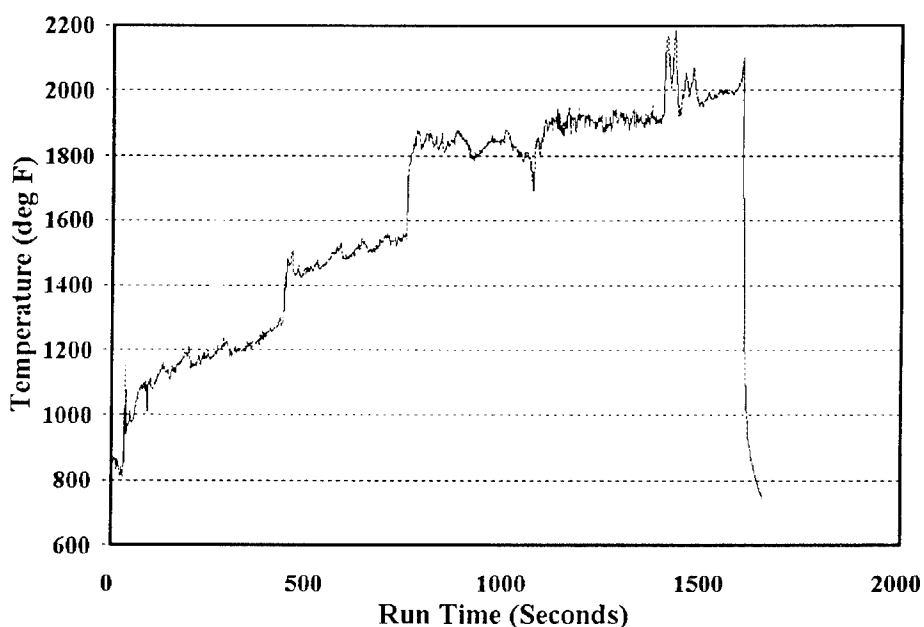


FIGURE 5-4: Experimental Exhaust Temperature

Regions where the exhaust gases and all structural components reached an equilibrium temperature were further developed to provide the required steady state values. The data within each time period of equilibrium was copied to a subsequent page of the spreadsheet file for manipulation. The temperatures were statistically analyzed at each measured point to provide the average value, standard deviation, and slope. If all of these values fell within acceptable ranges, the data was marked as a valid steady state reading and the temperature profile as a function of emitter position was plotted as in Figure 5-5 (McHenry, 1995).

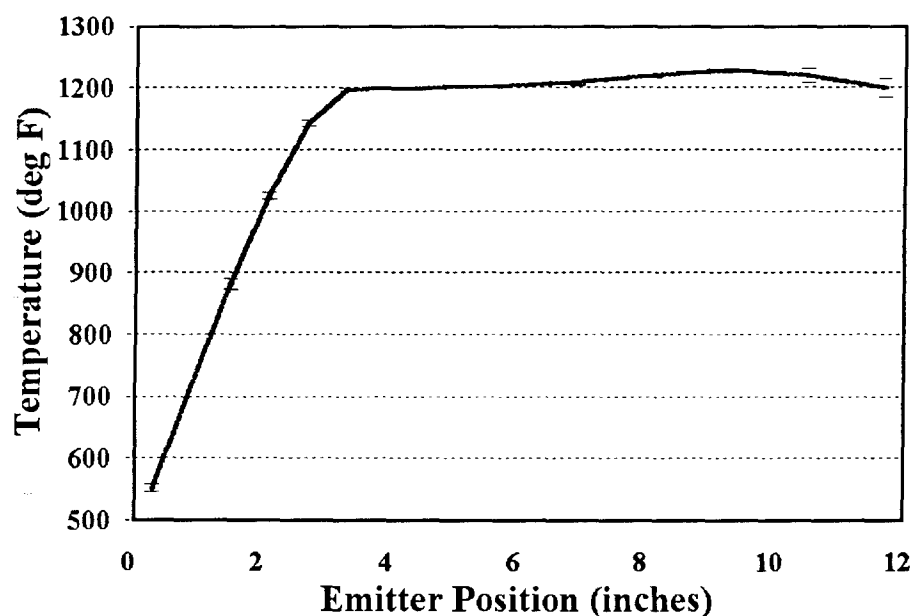


FIGURE 5-5: Experimental Temperature Profile

The final operational databank included data from 12 tests with air-to-fuel ratios ranging from 10 to 20, varying flow rates, and both glass and steel emitter tubes. It also included repeated flow conditions so that the accuracy of the readings could be evaluated. Temperature profiles for each run are included in the Appendix on pages 74-85. This databank provided the empirical history necessary to modify and validate the TPV computer program. The first phase of this process was the evolutionary development of the computer model discussed in Section 4.2. The program was continuously expanded until it considered enough different properties to maintain an accurate mathematical model of the operational prototype burner and was able to output realistic values for all of the calculated parameters.

Once the model reached this point of maturity, its predicted emitter temperature profile curves were plotted against each of the experimental data sets. This analysis demonstrated the accurate repeatability of the experimental data and also indicated that the model was in general accordance with the experimental values. Through iterative curve matching on all 12 experimental sets, a constant model configuration was determined which was suitable over the full range of materials and flow variation. It was determined that manipulation of the combustor efficiency number alone could be used to drive the predicted curves to very accurate agreement. This dependence of model curve matching on the combustor efficiency had a basis in the physical process within the TPV system. At the lower air-to-fuel ratios considered, the incomplete mixing of the combustion reactants caused combustion efficiencies in the 50% range. As the excess oxygen was increased at higher ratios, the combustion was more complete and efficiencies approached 75%. While these numbers were in general agreement with measured values in the literature, there was no standard predictive empirical or mathematical basis to determine the combustion efficiency. For this reason, the measured data of the prototype experimentation plan was used in conjunction with the TPV computer model predictions to generate a plot of combustor efficiency versus air-to-fuel ratio shown as Figure 5-6 (McHenry, 1995). This data distribution was then curve fitted to provide a linear function relating the two properties. (The sporadic data point at an air-to-fuel ratio of 14 had no known significance and was not included in the linear regression.) After inserting the regression equation into the computer model, it was reconverged at each of the 12 experimental steady states and the predicted and experimental curves were again compared, with excellent results.

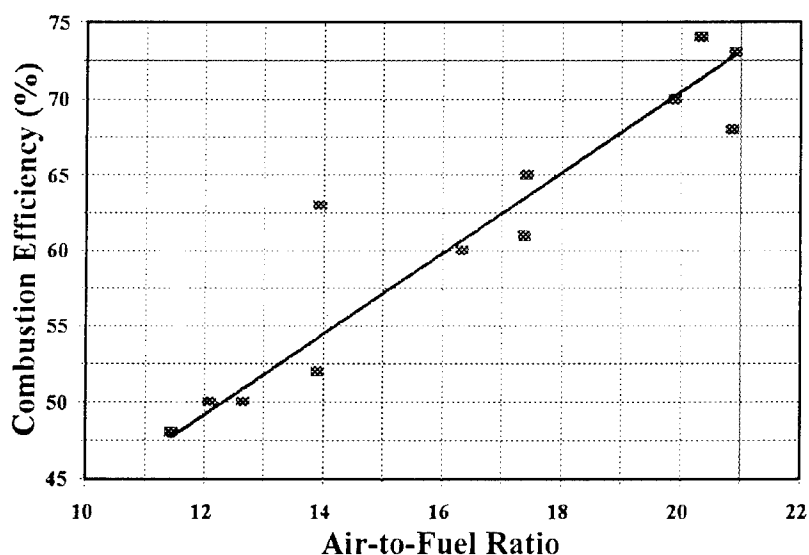


FIGURE 5-6: Combustor Efficiency Curve Fitting

6.0 PHASE IV: FINAL DESIGN

The ultimate objective of this project was the design of a combustion powered blackbody photon emitter to produce a uniform photon field incident to a selective spectral filter and thermophotovoltaic conversion cells. The design methodology resulted in the development of a TPV burner simulation computer program and prototype experimental data from which to synthesize an optimal final design. This design included a practical and optimal burner geometry, supporting materials considerations, and output control systems.

6.1 COMBUSTOR DESIGN

The first step in the completion of the project objectives was the determination of the burner's exact size, shape and configuration. The burner geometry was constrained by the required compatibility with the DOE TPV generator, the optimal combustion chamber size, and the availability of ceramic cylinders. The DOE TPV generator design was in flux throughout the project period, but was eventually solidified. The post photonic end of the generator developed off-site consisted of an array of photovoltaic cells coated with both a spectral filter and reflective backing to maximize conversion efficiency. This array was 8.00 inches long and was octagonal with 2.00 inch sides. The size of the TPV array established the upper bound of the emitter's outside diameter to be 4.83 inches. The inner dimension of the emitter cylinder was constrained by the combustion heating phenomenon. The emitter inner diameter determined the combustion reaction area, and this in turn controlled the flame characteristics and heat transfer. The larger the area of the cylinder, the lower the resultant emitter temperature would be given a constant fuel LHV and mass flow rate. A smaller emitter also meant a smaller reactant flow area and therefore higher flow velocity. Computer simulation and prototype operational experience indicated that the flow velocity criteria limited the inner diameter to a minimum of 3.00 inches. Finally, the cost effective procurement of ceramic components required the utilization of cylinder sizes that were standard in the industry. This limited the emitter cylinder to one inch increments of diameter with at least a one inch wall thickness. Given this set of constraints, the optimal emitter for the final design was determined to be 12.00 inches long with a 4.00 inch OD and a 3.00 inch ID. The 12.00 inch length was required to allow for the temperature profile ramp-up and drop-off so as to produce a constant photon energy region within the 8.00 inches covered by the TPV array.

The combustor's flame tube was engineered to produce the constant emitter temperature profile required. Its dimensions were constrained by the size of the emitter, the minimization of the combustion reactant flow velocity, the minimization of differential

pressure when material strengths begin to wane at high temperature, and the standard ceramics cylinder sizes. The size, flow and material requirements led to the selection of a 12.00 long, 1.00 inch wide high purity alumina flame tube. This size was commonly available and offered sufficiently large flow area to make the flow rates acceptable. The remainder of the flame tube design involved the location of the fuel flow holes drilled through its surface. Placement of the fuel hole locations had a rather dramatic effect on the resultant emitter temperature profile by manipulating the mass flow of fuel for combustion at each point along the length. The computer simulation software was used extensively to optimize the system performance given varied hole configurations. This optimization process involved the variation of the hole sizes and locations over the full range of reasonable values. The computer predictions for each configuration were plotted and the most linear portion of the emitter profile was analyzed using its slope and standard deviation. The final result was that sixteen 0.075 inch diameter holes drilled radially 0.300 inches from the bottom of the flame tube, followed by four 0.020 inch holes drilled every 0.600 inches for the rest of its length, generated an emitter temperature profile with a 0.76 degree per inch slope and only 3 degree variation. The computer generated performance curve for the optimal combustor geometry is displayed in Figure 6-1 (McHenry, 1995).

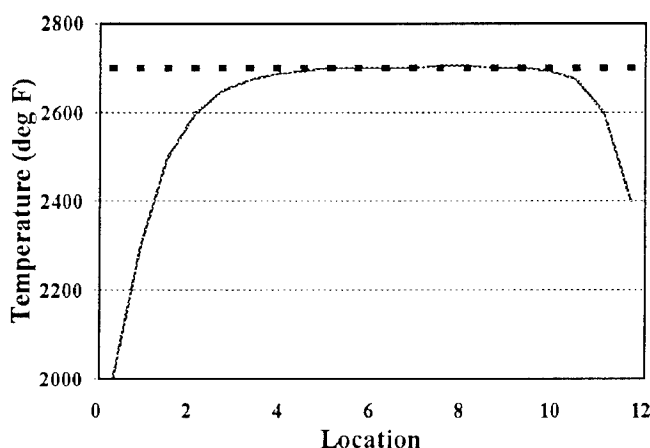


FIGURE 6-1: Predicted Emitter Temperature Profile

In order to support the emitter and flame tube cylinders and to generate the coaxial combustion reactant flow, three fluid headers were needed. The first of these was the fuel header which accepted the inlet fuel hose and conveyed the fuel to the inside of the flame tube. The second was an air header which accepted the inlet air and distributed it coaxially around the flame tube to support the combustion reaction. The third was the exhaust header which collected the combustion product gases and channeled them to the exhaust duct. There

were no physical constraints on the size of these headers, other than a minimum size to contain the necessary flow paths and the standard size requirement to ease in procurement. The final design utilized identical ceramic disks as the base for each of these headers, with the specific flow paths required for each drilled out of the base piece. This approach decreased procurement costs and reduced the complexity of the design. The final base header disks were 5.00 inches in diameter and 3.00 inches tall. Figure 6-2 on page 50 (McHenry, 1995) is a sketch of the combustor design.

6.2 BALANCE OF PLANT REQUIREMENTS

With the combustor geometry defined, the balance of plant requirements to construct a fully operational photon emission system were completed. The computer modeling process verified that a recuperative heat exchanger was necessary to achieve the target emitter temperature and increase the cycle efficiency. This recuperation used the high temperature exhaust gases to preheat the inlet air so that higher temperatures could be sustained by the combustion process at lower fuel flow rates. Attempts to research the procurement of a suitable heat exchanger revealed the fact that the TPV combustion system exceeds the capabilities of commercially produced units (Coubrough, 1988 and personal communications). Very few heat exchangers could withstand even 50% of the projected exhaust stream temperature and of those, none were of an appropriate size for incorporation into the system. An extremely simple high temperature heat exchanger was then designed and built in-house. It consisted of a 22.00 by 10.00 by 18.00 inch stainless steel shell with inlet and outlet fittings for the exhaust gases and combustion air. The top of this shell was gasket sealed and allowed for the insertion of ceramic plates. Four plates were used to insulate the inner surfaces of the steel box in order to protect them from the high temperatures and reduce thermal losses. Two additional plates were inserted into grooves down the middle of the box to form three separated chambers. The hot exhaust gases flowed into the center chamber, heated the ceramic plates and were exhausted at a cooler temperature. The inlet air flowed through the outer two chambers, received the heat from the ceramic plates, and entered the combustor at an elevated temperature. While this design was very primitive compared to commercial recuperators, it met the high temperature requirements and was simple enough to allow for in-house construction. The simple design was adequate due to the fact that even at only 50% effectiveness in operation it would produce preheated combustion air at more than 1500°F and would more than fulfill its intended role. Figure 6-3 on page 51 (McHenry, 1995) is a sketch of the combustor-heat exchanger system.

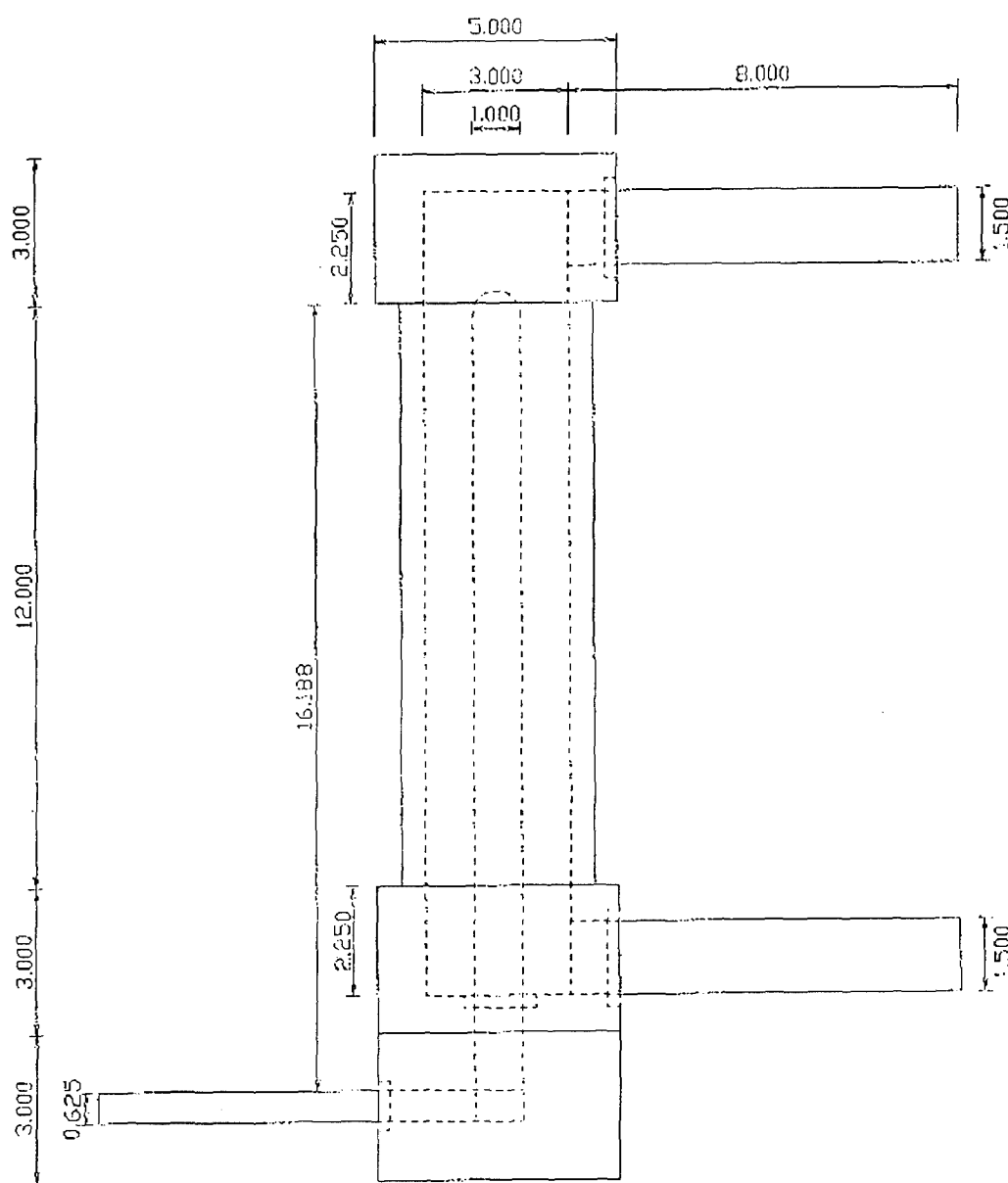


FIGURE 6-2: FINAL TPV COMBUSTOR DESIGN

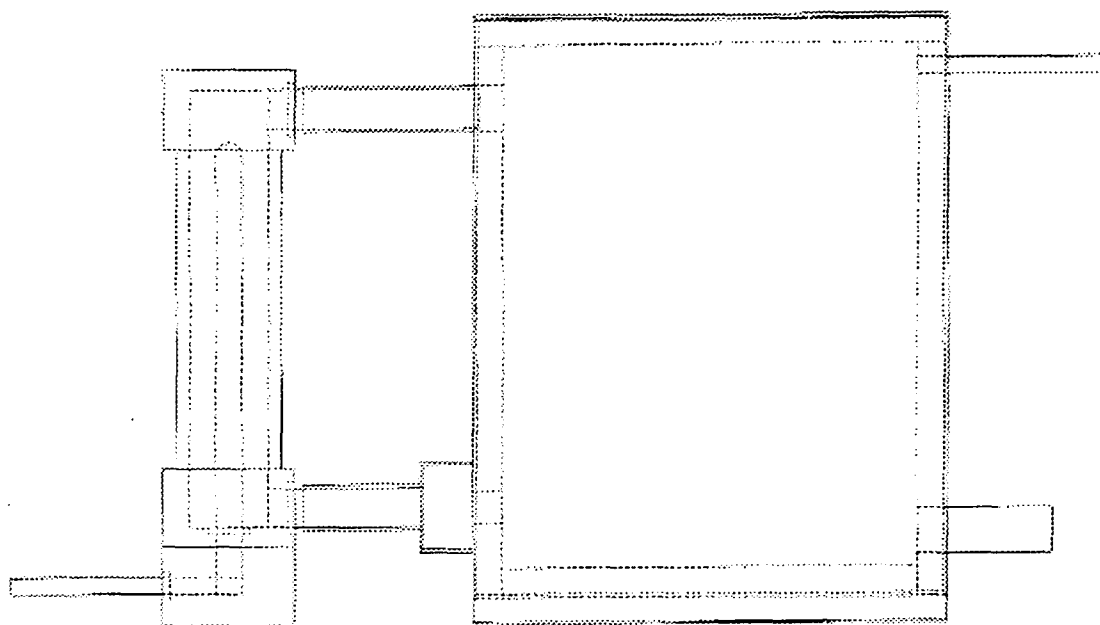


FIGURE 6-3: Combustor and Heat Exchanger Designs

The final requirement for the completed combustor system was a method to control the photon energies by controlling the combustion process more precisely. In the prototype experimentation, which used simple valves and variable area rotameters to control and measure the gas flow rates, it was very difficult to accurately reach target temperatures. The valves did not offer enough precision and the changing tank pressures required continuous adjustment to maintain constant flow rates. This resulted in the inability to reach and hold steady state conditions due to the dynamics of the flow conditions. The solution incorporated into the final design was to replace both the valves and rotameters with electronic mass flow controllers. These devices measured the actual mass flow rate of the gas without the need for temperature and pressure compensation, and contained set point solenoid valves to maintain constant downstream flow rates despite upstream variation. With these controllers installed, the user could set a simple knob to a tabulated value corresponding to the exact temperature and photon energy desired.

Once the entire system was designed, it was input into the computer model for further analysis. Specifically, the model was used to determine the maximum operational temperatures developed by each component. These temperatures were subsequently used to select the component materials from those discussed in Chapter 3. The silicon carbide, zirconia and Alcoa CA-25 calcium aluminate were all used for emitter tubes to allow for experimentation in survivability and photon emission spectrum. The ceramic for the air

headers was selected to be an alumina compound sold by the Zircar Company. The ceramic sheets required within the heat exchanger were alumina as well and were procured from the Rath Performance Fiber Company. The remainder of the system components consisted of stainless steel and rubber tubing, steel fittings and valves, and two mass flow controllers purchased from Porter Instruments.

7.0 CONCLUSIONS

This Trident Scholar research project conducted at the U.S. Naval Academy accomplished its objectives as outlined in the governing DOE interagency agreement. This section provides a final overview of the photon emitter design, evaluates the design against the initial objectives, and offers a summary of the significant results and conclusions generated by the project.

7.1 DESIGN EVALUATION

The specifications of the completed USNA TPV photon emitter system are listed below in Table 7-1.

TABLE 7-1: Complete Design Specifications

1. Emitter Cylinder
 - Silicon Carbide, Zirconia, and Calcium Aluminate Mortar
 - 12" Long, 4" OD, 3" ID
 - 2700°F Surface Temperature
 - Near Blackbody Emittance
 2. Flame Tube
 - High Purity Alumina
 - 12" Long, 1" OD, 0.75" ID
 - 3500°F Operational Temperature
 3. Flow Headers
 - Alumina
 - 3" Long, 5" OD
 - 3000°F Operational Temperature
 4. Heat Exchanger
 - Stainless Steel, Alumina, Silicon Carbide
 - 18" x 22" x 10" Steel Shell
 - 1" Thick Insulation
 - 0.25" Thick Transfer Surface
 - 4.5 ft² of Transfer Area
 - 50% Target Effectiveness
-

With the full engineering design of the TPV emitter system completed, it was evaluated against the initial project objectives and the provisions of Interagency Agreement DE-A112-94SN39277. Table 7-2 lists the original DOE objectives and the final design's ability to meet them.

TABLE 7-2: Evaluation of Initial Objectives

DOE OBJECTIVE	YES	NO
Geometrically Compatible with DOE TPV Generator System	X	
Uniform 2700°F Photon Emission Temperature	X	
Near Blackbody Photon Emission Characteristics	X	
Portable and Completely Self Sufficient	X	
Optimized Cycle Efficiency	X	
Optimal Fuel Selection	X	
Gas Burner Design and Optimization	X	
Flame and Temperature Control	X	
Thermally Suitable System Materials	X	
Development of Computer Simulation Software	X	

The USNA TPV photon emitter system meets or exceeds all of the initial design specifications. The final apparatus is very simple, inexpensive (with a total cost under \$10,000), and suitable for continued experimentation with the TPV process. It allows the researcher to demonstrate self-contained TPV electrical generation in a portable package. It also has value in continuing laboratory work due to its variable emission temperatures. This temperature range can be used to test existing cell efficiencies and to allow the system to be used with the lower band-gap cells to be developed in the future. The TPV emitter's ability to meet the apparatus requirements, the relatively inexpensive design, and the value to TPV research warrant that this project be continued to the full construction phase and that

the USNA TPV emitter be put into operational use as the power core of the DOE TPV generator.

7.2 PROJECT RESULTS

Completion of the U.S. Naval Academy TPV photon resulted in the following research products:

1. A comprehensive report describing the nature of the thermophotovoltaic energy conversion process and important supporting technologies. Of particular interest are the proposed concepts for the incorporation of TPV systems into a wide variety of commercial and military applications (Section 2.4) and the high temperature materials summary for ceramic mortars (Section 3.3).
2. A detailed computer model of the TPV combustor system which accepts user-defined geometries and combustion reactions, and iteratively solves the complex system of controlling equations and outputs critical performance properties (Section 4.2). This computer model has been empirically validated through experimentation and is capable of predictive design optimization (Section 5.4).
3. The complete engineering design of an operational photon emission system which satisfies the research objectives by developing a uniform 2700°F near blackbody photon emission surface over a 12 inch long and 4 inch outer diameter ceramic cylinder. This emitter system is contained in a portable unit including compressed air and methane fuel sources, a recuperative heat exchanger, and set point photon energy control (Chapter 6).

7.3 PROJECT CONCLUSIONS

1. The concept of TPV energy conversion has been the subject of significant research efforts over the past thirty years and there exists a broad base of theoretical and practical knowledge. This technology is currently cost effective in a limited number of specific applications, and, with future development, has great potential for wide application within the power industry.
2. There are a number of gaseous fuels that could be used within a combustion powered TPV generator. Methane proved to have the highest LHV, the lowest cost, and the widest availability.
3. The high temperature materials problems of previous TPV work can be overcome by current commercial ceramics technology. The ceramics industry has matured to the point that cost effective ceramic materials with outstanding high temperature properties are readily available and reliable. These are primarily silicon carbide, high purity alumina, and partially

stabilized zirconia. There are also a number of ceramic mortar compounds which offer a low cost, in-house alternative to full ceramic procurement.

4. A complete computer representation of the TPV process can produce accurate results and be used for predictive engineering design optimization.
5. Methane combustion can be controlled and manipulated so as to determine the peak energy of the photon spectrum emitted. Careful combustor design will ensure stable combustion properties and minimize deviation from a constant temperature profile.
6. The key properties of the emitter material, beyond the ability to withstand the thermal requirements, are the emissivity and conductivity. Emissivity values approaching unity are critical for system efficiency and power density, and high conductivity is important to achieve a flat temperature profile.
7. Recuperative heat exchangers are necessary for the efficient operation of a TPV generator. Currently available heat exchangers offer little application to this process, although a simple high temperature unit can easily be built and should perform satisfactorily.

REFERENCES

- Avallone, Eugene and Theodore Baumeister. Marks' Standard Handbook for Mechanical Engineers. 9th ed. New York: McGraw Hill, 1987.
- Angrist, Stanley. Direct Energy Conversion. 3rd ed. New York: McGraw Hill, 1988.
- Apriainen, Matti, et al. "Naval Architecture of Electric Ships - Past, Present and Future." The Society of Naval Architects and Marine Engineers. Jersey City, New Jersey. September 1993.
- Barnard, J.A. and J.N. Bradley. Flame and Combustion. 2nd ed. London: Chapman and Hall, 1985.
- Belkhatay, Mohammed. "Thermophotovoltaic (TPV) Energy Generation for Navy Ships and Submarines, Technology Survey." Document # CDNSWC-TM-80-93-7. Propulsion and Auxiliary Systems Department. Naval Surface Warfare Center, Carderock Division, Annapolis Detachment, Bethesda, Maryland. February 1993.
- Block, Leo et al. "Thermophotovoltaics: A New Cogeneration Technology for Gas Appliances." IEEE Transactions on Industry Applications, Vol. 28, No. 1. January 1992.
- Chubb, Donald, and Dennis Flood. "High Efficiency Thermal to Electric Energy Conversion Using Selective Emitters and Spectrally Tuned Solar Cells." Document # NASA-TM-105755. National Aeronautics and Space Administration, Cleveland, Ohio. August 1992.
- Chubb, Donald, and Dennis Flood. "High Efficiency Thermal to Electric Energy Conversion Using Selective Emitters and Spectrally Tuned Solar Cells." Document # NASA-TM-106227. National Aeronautics and Space Administration, Cleveland, Ohio. August 1993.
- Compressed Gas Association. Handbook of Compressed Gases. 2nd ed. New York: Van Nostrand Reinhold, 1981.
- Coubrough, Lawrence et al. "Compact Ceramic Heat Exchangers." Document # GRI-88/0172. Prepared by Coors Ceramics Co. for the Gas Research Institute, Chicago, IL. June 1988.
- Dehlsen, James. United States Patent #5,066,339. November 1991.

REFERENCES (Continued)

- Duomarco, Jose, and Roy Kaplow. "Theoretical Estimations of the Efficiency of Thermophotovoltaic Systems using High-Intensity Silicon Solar Cells." Solar Energy. Vol. 32, No. 1, 1984: 33-40.
- Fritz, Sandy. "Hybrid Vehicles: Burning the Midnight Sun." Popular Science. February 1995: 29.
- Guazzoni, Guido. "High-Temperature Spectral Emittance of Oxides of Erbium, Samarium, Neodymium, and Ytterbium." Applied Spectroscopy. Vol. 26, Article 1: 1971.
- Guazzoni, Guido, and B. Pizzo. "Hybrid Thermophotovoltaic Power Sources." Electronics and Power Sources Directorate. Army Research Laboratory, Ft. Monmouth, New Jersey.
- Guazzoni, Guido. Army Research Laboratory, Ft. Monmouth, New Jersey. Telephone and Facsimile Correspondance: 1995
- Kazimierzak, B. et al. "An ODS Material with Outstanding Creep and Oxidation Properties above 1100 C." Key Engineering Materials Vol. 77-78: 363-74.
- Kittl, E. and Guido Guazzoni. "Design Analysis of TPV-Generator System." 25th Annual Proceedings Power Sources Conference - May, 1972. May 1972
- Kleiner, R. and L. Coubrough. "Compact Ceramic Heat Exchangers." Document # GRI-88/0172. Coors Ceramic Company for Gas Research Institute, Chicago, Illinois. June 1988.
- Kotchick, David. "High Temperature Mechanical Properties of Sintered Alpha Silicon Carbide." AIRsearch Manufacturing Co. for the Office of Naval Research, Department of the Navy. December 1978.
- Kreith, Frank and Mark Bohn. Principles of Heat Transfer. 5th ed. St. Paul, Minnesota: West Publishing, 1993.
- Levy, S.L., and N.G. Galluzzo. "Thermophotovoltaic Conversion From Conventional Heat Sources." Document # ER-1262. Black & Veatch Consulting Engineers for Electric Power Research Institute, Palo Alto, California. December 1979.
- Lindeburg, Michael. Engineer-in-Training Reference Manual. 8th ed. Belmont, California: Professional Publications, 1992.

REFERENCES (Continued)

Lindler, Keith. USNA TPV. Vers. 1.0. Computer Software. U.S. Naval Academy, 1995. Quattro Pro® for Windows 5.0 or higher 901K, disk.

McHenry, Robert. "The Design and Construction of a High Temperature Photon Emitter for a Thermophotovoltaic Generator." Trident Scholar Report. U.S. Naval Academy. May 1995.

Moeller, Helen. "SiC Fiber Reinforced SiC Composites Using Chemical Vapor Infiltration." SAMPE Quarterly, Vol. 17 No. 3, April 1986.

Nelson, Robert. "Fibrous Emissive Burners Selective and Broad Band." Document # TR4527-029-93. Tecogen for Gas Research Institute, Chicago, Illinois. October 1993.

Nelson, Robert. United States Patent #5,057,162. October 1991.

Omega Temperature Measurement Handbook and Encyclopedia. Stamford, Connecticut: Omega Engineering Inc., 1992.

"Pocket Engineering Guide." Rockford, Illinois: Eclipse Inc., 1971.

Rorabaugh, Michael and David Mann. "Advanced Silicon Carbide Heat Exchanger Materials." SAMPE Quarterly, Vol. 9. April 1978: 44-9.

Schwartz, Mel. Handbook of Structural Ceramics. New York: McGraw Hill, 1992.

Somiya, Shigeyuki. Advanced Technical Ceramics. Tokyo: Academic Press, 1989.

Valenti, Michael. "Keeping the Home Fires Burning." Mechanical Engineering July 1993: 66-69.

"Zircar Fibrous Ceramics." Florida, New York: Zircar Products Incorporated, 1995

APPENDIX

<u>TITLE</u>	<u>PAGE</u>
Fuel Analysis Calculations	61
System Schematic	65
Prototype Component Engineering Sketches	66
Exhaust Hood Design	71
Standard Operating Procedures	72
Experimental Emitter Temperature Profiles	74
Heat Exchanger Engineering Sketch	86

HEATING VALUE AND FLAME TEMPERATURE OF FUELS

Heating Value of Fuels

The heating value of a fuel is calculated as the heat that would be released if the products of combustion are cooled back to standard temperature and pressure (298 K, .1 MPa). It can be expressed in terms of the heat of formation of the reactants and products of combustion. The lower heating value (LHV) is obtained if the water in the products is assumed to be a vapor.

$$LHV = \sum n_F \bar{h}_R - \sum n_P \bar{h}_P \quad (1)$$

For example, to find the heating value of methane, first write the balanced chemical equation.



From equation 1, the heating value would be calculated as:

$$LHV(CH_4) = (1) \bar{h}_f^\circ(CH_4) + (2) \bar{h}_f^\circ(O_2) - (1) \bar{h}_f^\circ(CO_2) - (2) \bar{h}_f^\circ(H_2O) \quad (3)$$

Substituting in the heat of formations for the reactants and products:

$$LHV(CH_4) = (1)(-74,873) + (2)(0) - (1)(-393,522) - (2)(-241,826) \quad (4)$$

$$LHV(CH_4) = 802,301 \text{ kJ/kmol fuel} \quad (5)$$

To calculate the LHV per mass of fuel, divide the molal value by the molar mass of the fuel:

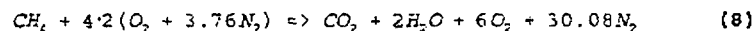
$$LHV(CH_4) = \frac{802,301 \text{ kJ}}{\text{kmol fuel}} \frac{\text{kmol fuel}}{16.043 \text{ kg fuel}} = 50009 \text{ kJ/kg fuel} \quad (6)$$

Thus the products of combustion include 7.52 moles of nitrogen in addition to the one mole of carbon dioxide and 2 moles of water vapor. The heating value of the fuel is now used to heat the 7.52 moles of nitrogen as well as the carbon dioxide and water vapor thus resulting in a much lower flame temperature of 2329 K.

Table 2. Spreadsheet for calculating the adiabatic flame temperature for various combustion products.

T (K)	Enthalpy (kJ/kmol)				Products of CH ₄ burned in pure oxygen
	h (N ₂)	h (O ₂)	h (CO ₂)	h (H ₂ O)	
298	0	0	0	0	0
300	54	54	69	62	193
400	2971	3027	4003	3450	10903
500	5911	6085	8305	6922	22149
600	8894	9245	12906	10499	33904
700	11937	12499	17754	14190	46134
800	15046	15836	22806	18002	58810
900	18223	19241	28030	21937	71904
1000	21463	22703	33397	26000	85397
1100	24760	26212	38885	30190	99265
1200	28109	29761	44473	34506	113485
1300	31503	33345	50148	38941	128030
1400	34936	36938	55895	43491	142877
1500	38405	40600	61705	48149	158003
1600	41904	44267	67569	52907	173383
1700	45430	47959	73480	57757	188994
1800	48979	51674	79432	62693	204818
1900	52549	55414	85420	67706	220832
2000	56137	59176	91439	72788	237015
2200	63362	66770	103562	83153	269868
2400	70460	74453	115779	93741	303261
2600	77963	82225	128074	104520	337114
2800	85323	90080	140435	115463	371361
3000	92715	98013	152853	126548	405949
3200	100134	106022	165321	137756	440833
3400	107577	114101	177836	149073	475982
3600	115042	122245	190394	160484	511362
3800	122526	130447	202990	171981	546952
4000	130027	138705	215624	183552	582728
4400	145078	155374	240992	206892	654776
4800	160188	172240	266488	230456	727400
5200	175352	189312	292112	254216	800544
5600	190572	206618	317870	278161	874192
6000	205848	224210	343782	302295	948372

The flame temperature can be controlled by combusting with excess air. For example if the methane is combusted with 4 times the amount of air that is necessary, the balanced chemical equation would be:



The heating value of the fuel is now used to heat the 6 moles of excess oxygen and 30.08 moles of nitrogen in addition to the carbon dioxide and water vapor. The resulting flame temperature is 951 K.

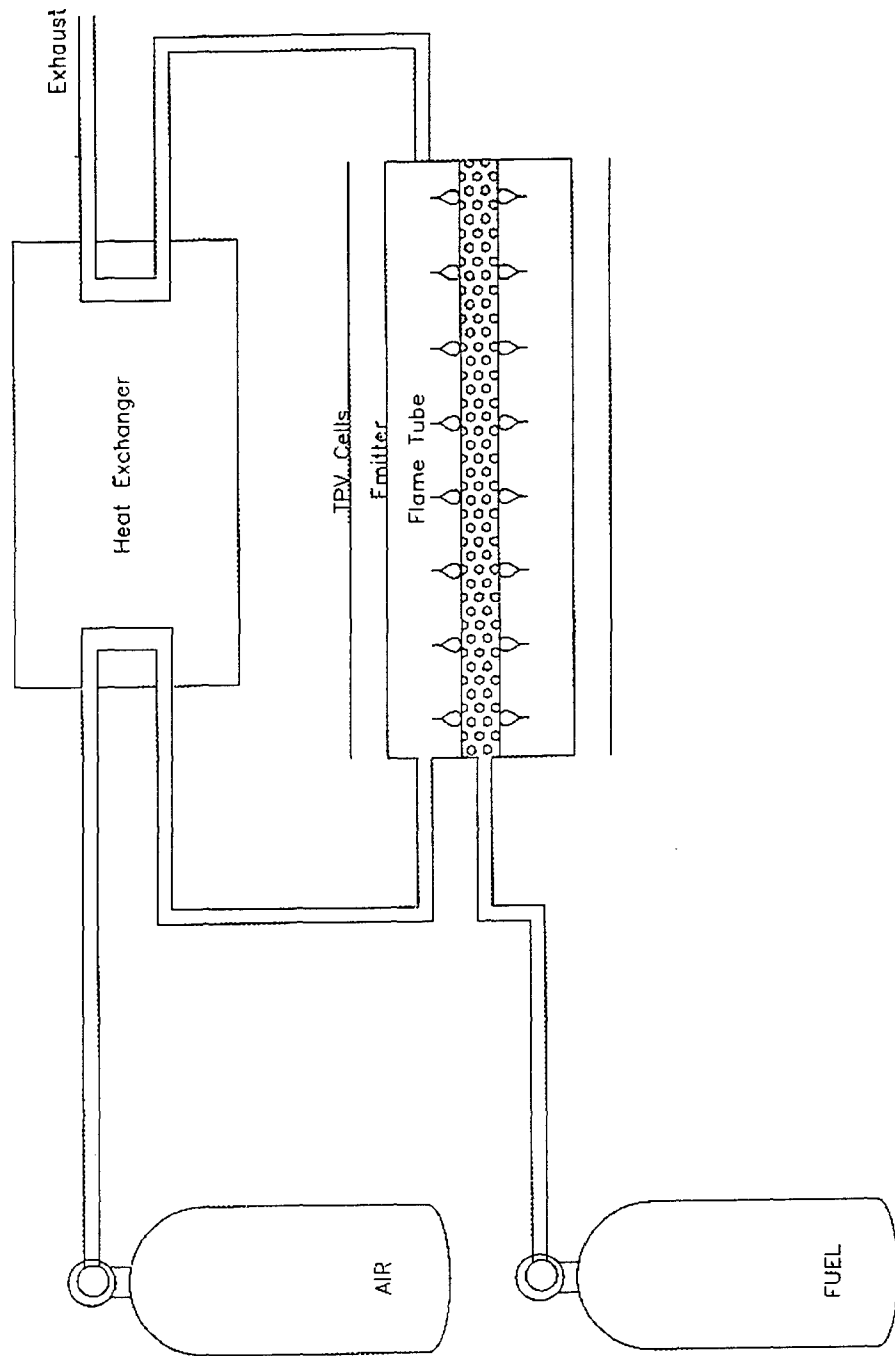
The spreadsheet was used to calculate the flame temperatures for all of the fuels listed in table 1. The results are shown in table 3 (degrees K) and table 4 (degrees F).

Table 3. Adiabatic flame temperatures for various fuels (K)

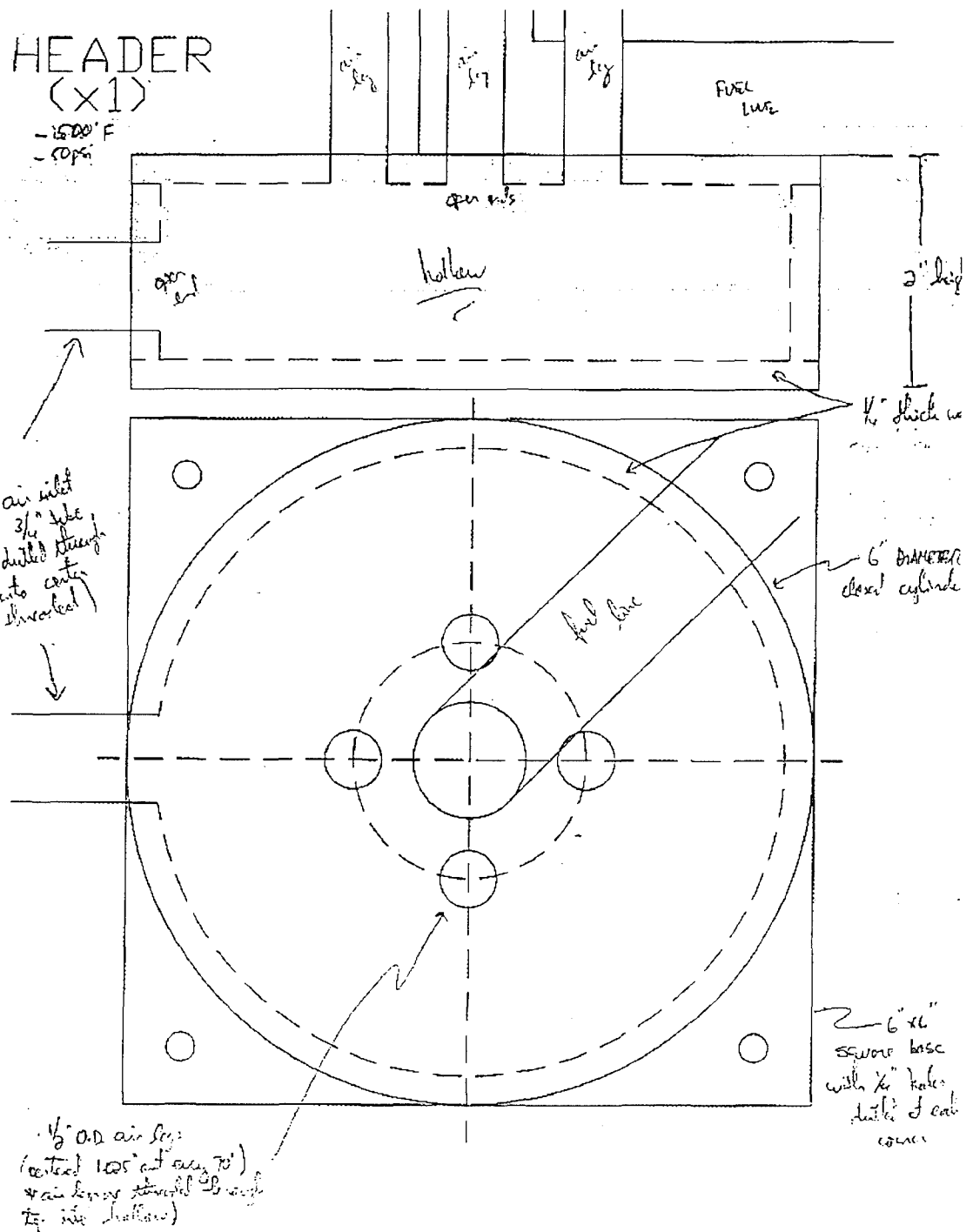
Flame Temperatures (K)			
Fuel	Pure Oxygen	100% Air	400% Air
Hydrogen	5095	2526	1059
Methane	5210	2329	951
Acetylene	7400	2909	1112
Ethene	6124	2567	1016
Ethane	5462	2384	963
Propene	5967	2508	996
Propane	5548	2397	965
Butane	5591	2402	965
Pentane	5620	2406	966
Benzene	6351	2530	992
Hexane	5640	2409	966
Heptane	5654	2411	967

Table 4. Adiabatic flame temperatures for various fuels (°F)

Flame Temperatures (°F)			
Fuel	Pure Oxygen	100% Air	400% Air
Hydrogen	8711	4087	1446
Methane	8918	3732	1252
Acetylene	12860	4776	1542
Ethene	10563	4161	1369
Ethane	9372	3831	1273
Propene	10281	4054	1333
Propane	9526	3855	1277
Butane	9604	3864	1277
Pentane	9656	3871	1279
Benzene	10972	4094	1326
Hexane	9692	3876	1279
Heptane	9717	3880	1281



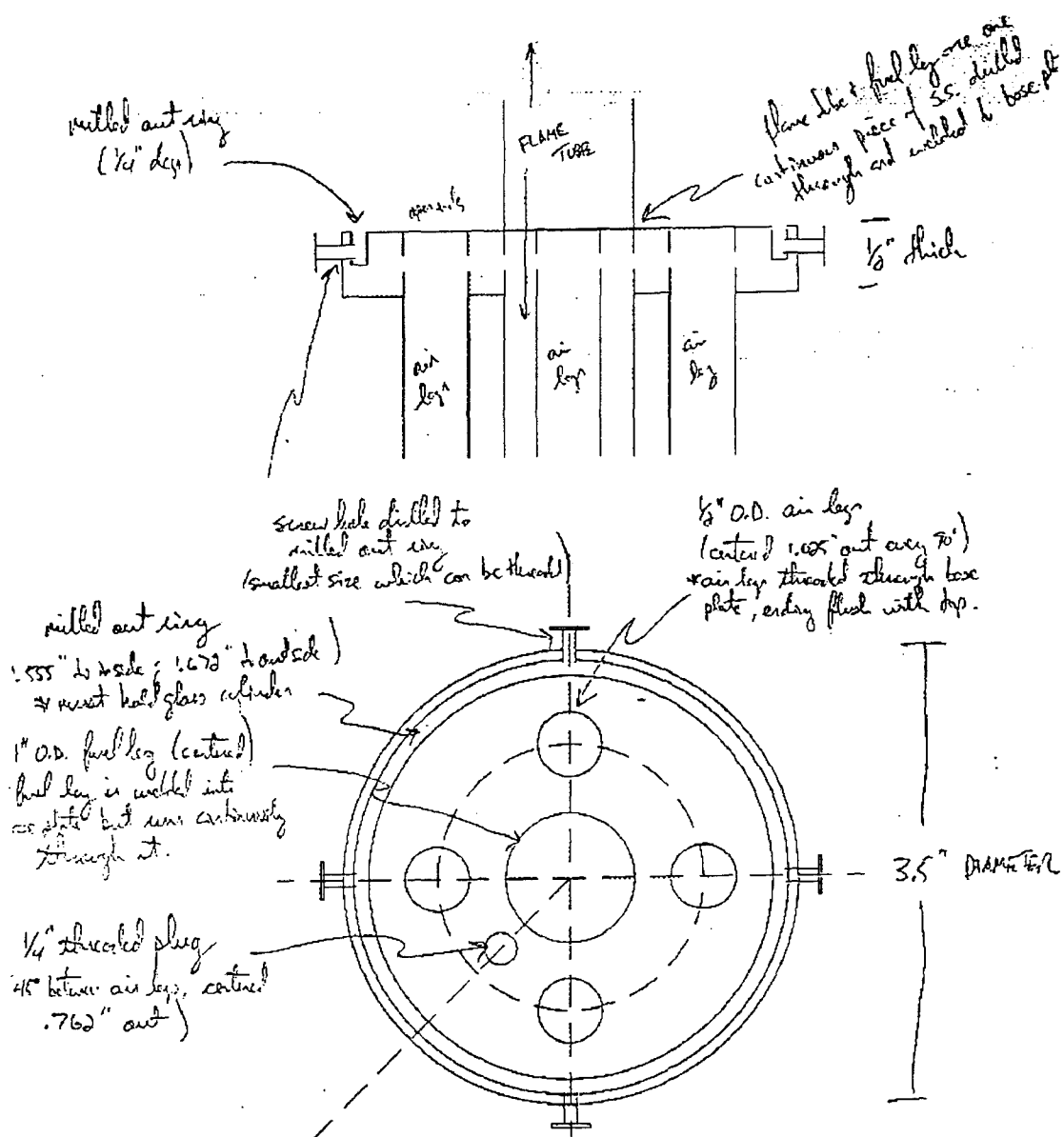
Conceptual System Schematic



Prototype Air Header

BASE PLATE (X1)

-1500°F
-50psi

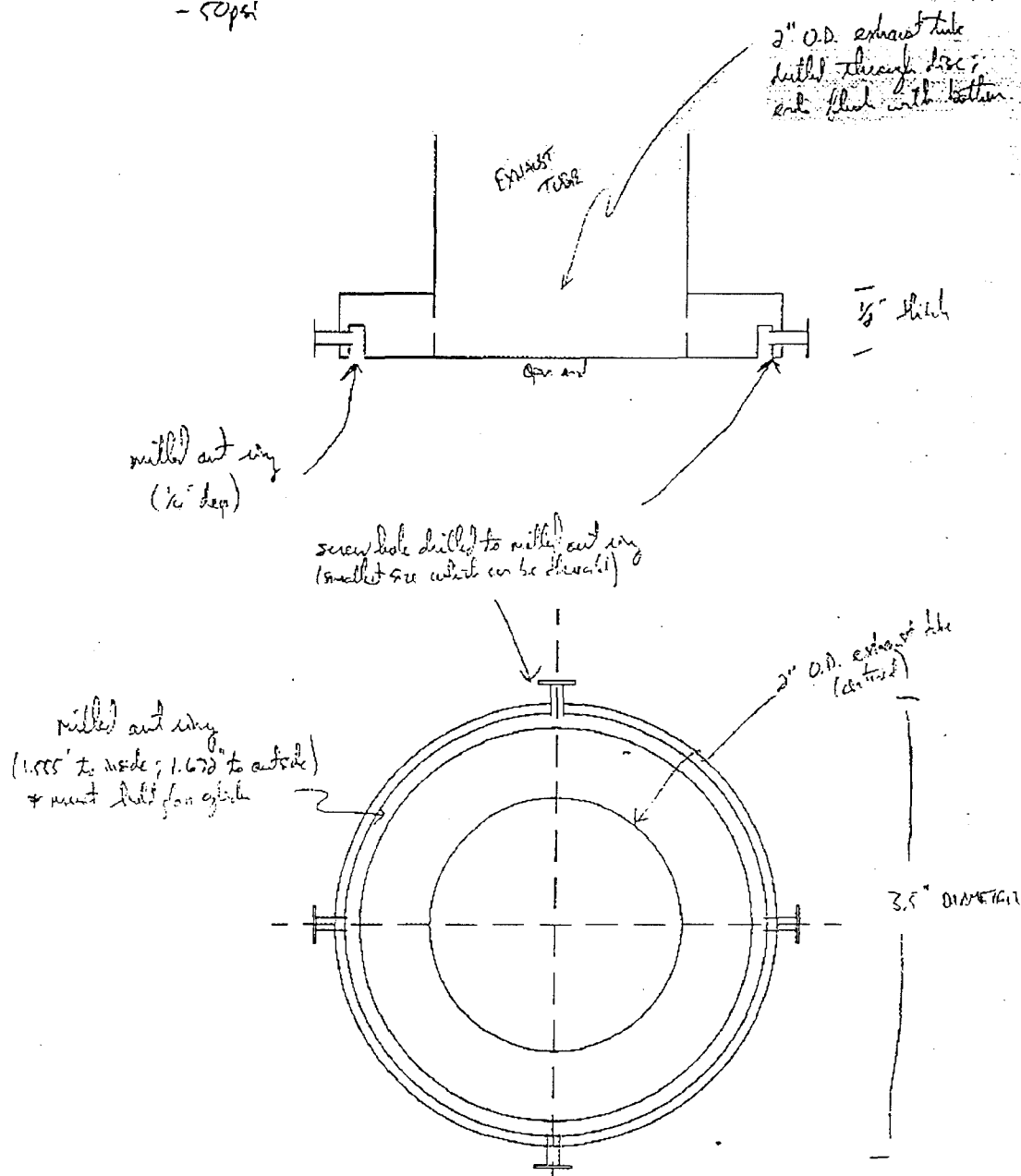


Prototype Base Plate

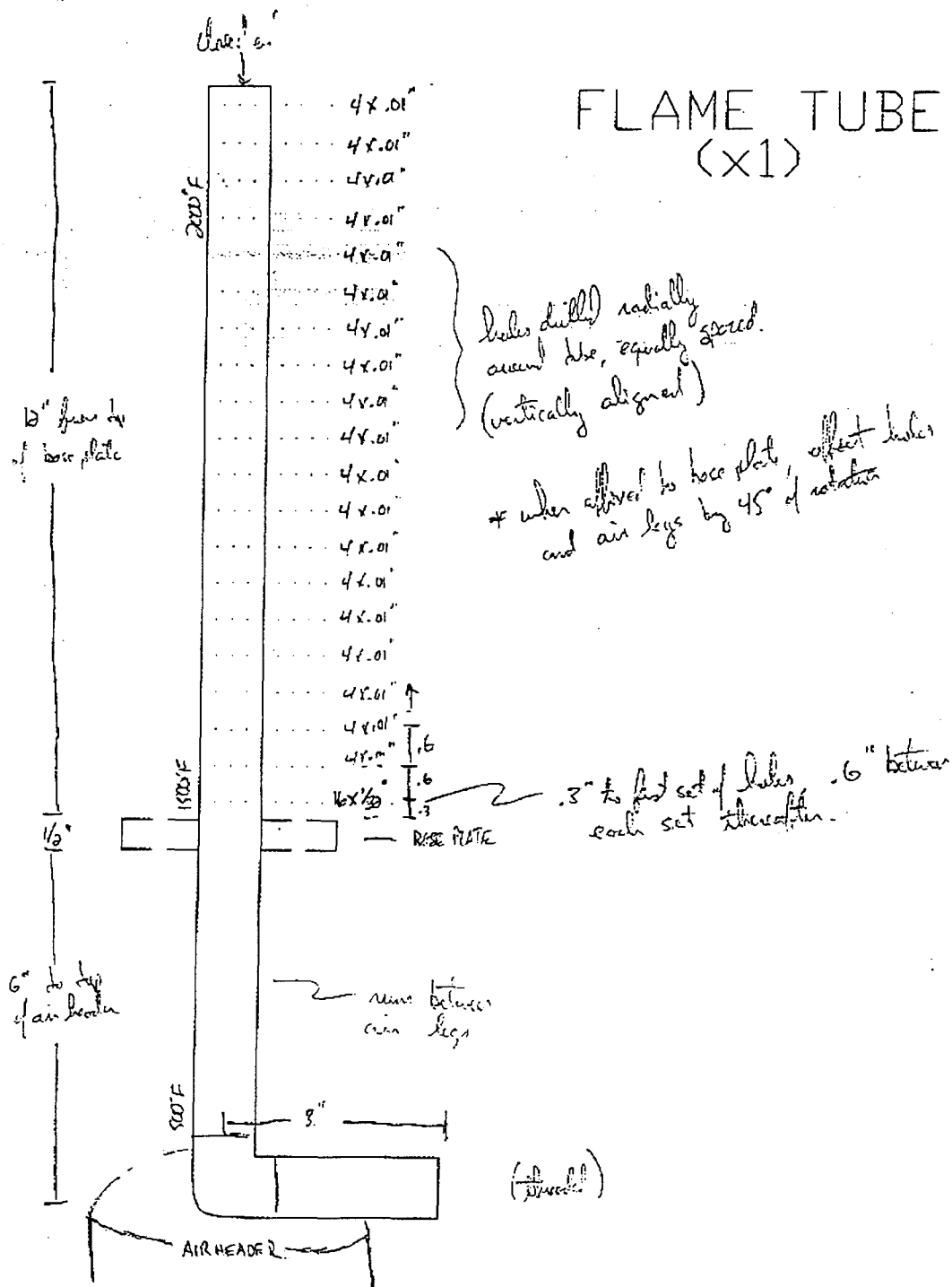
TOP PLATE (x1)

- 200°F

- 50 psi



Prototype Top Plate



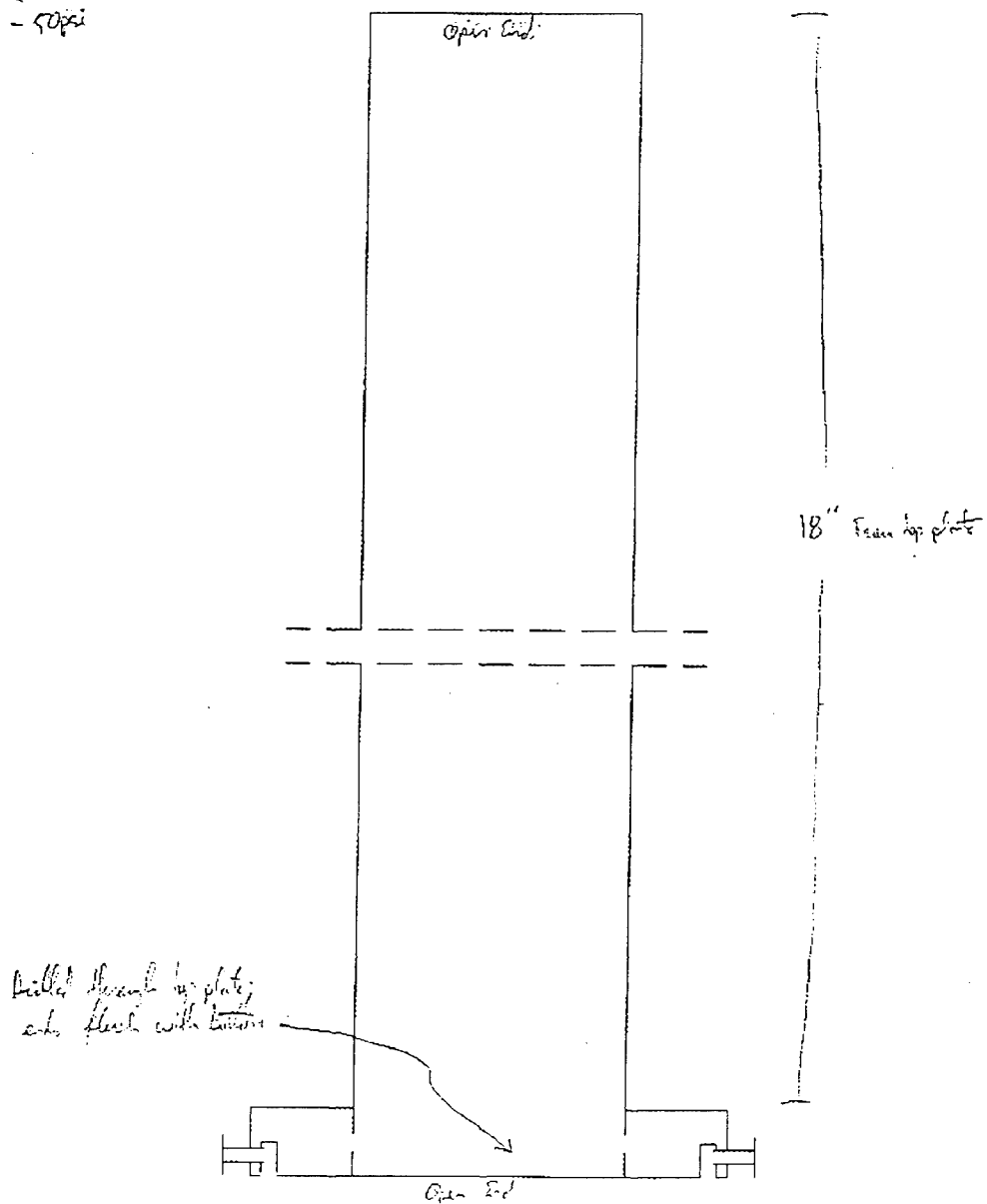
Prototype Flame Tube

EXHAUST TUBE (x1)

- 2000°F

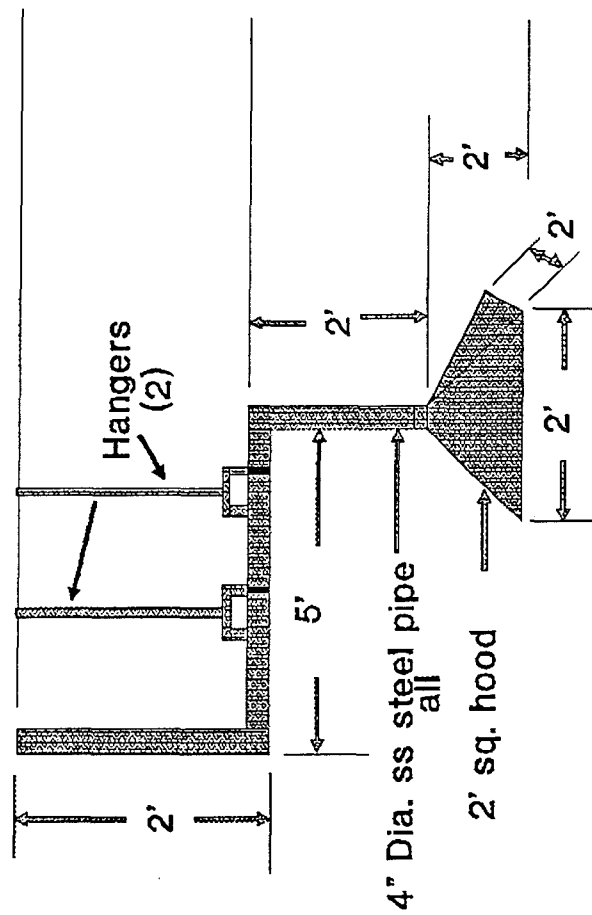
- 50psi

1 2" O.D. Tube 1



Prototype Exhaust Tube

EXHAUST SYSTEM FOR TRIDENT PROJECT



Hood to be approx. 6' off floor

Test Cell Exhaust Duct

Trident Project
OPERATING PROCEDURES:

OPERATOR: _____

DATE: _____ TIME: _____

TARGETS: Temp _____ FA-1 _____ FG-1 _____

1. PERSONNEL

- ☐ Clear uninvolved personnel
- ☐ Familiarization with apparatus and procedures
- ☐ Eye Protection

2. TEST CELL PREPARATION:

- ☐ Close test cell doors
- ☐ Clear immediate area of clutter and flammables
- ☐ Activate exhaust fan, verify unobstructed ducting
- ☐ Place thermal gloves on workbench

3. PRE-IGNITION LINE-UP:

- ☐ Verify thermocouple contacts
- ☐ Set computer clock to watch time
- ☐ Activate data logging file and save system setup
- ☐ Power down computer (ensure empty drive a:)
- ☐ Close valves VA-3 (CW), VG-3 (OL), VG-2 (CCW)
- ☐ Open valves VA-1 (CCW) and VG-1 (CCW)
- ☐ Record PA-1 and PG-1

4. IGNITION:

- ☐ Open valve VA-3 (CCW) until FA-1 reads (20)
- ☐ Open valve VG-3 (IL)
- ☐ Open valve VG-2 (CW) until FG-1 reads (5)
- ☐ Press ignition switch repeatedly until ignition
- ★ IF IGNITION DOES NOT OCCUR WITHIN (5) SECONDS, CLOSE VALVE VG-3 FOR (10) SECONDS BEFORE REPEATING!

5. DATA COLLECTION:

- ☐ Power up computer, wait for data logging
- ☐ Open valve VG-2 (CW) until FG-1 reads (10)

- ☐ Open valve VA-3 (CCW) until FA-1 reaches target
- ☐ Open valve VG-2 (CW) until FG-1 reaches target
- ★ Fuel may need to be increased incrementally with air flow to prevent instability and blowout.
- ☐ Record PA-3 and PG-3 _____ /
- ★ Maintain target flow readings by adjusting VA-3 and VG-2
- ★ Continue until steady state ($< 5^{\circ}\text{F}/\text{min}$ variation) _____

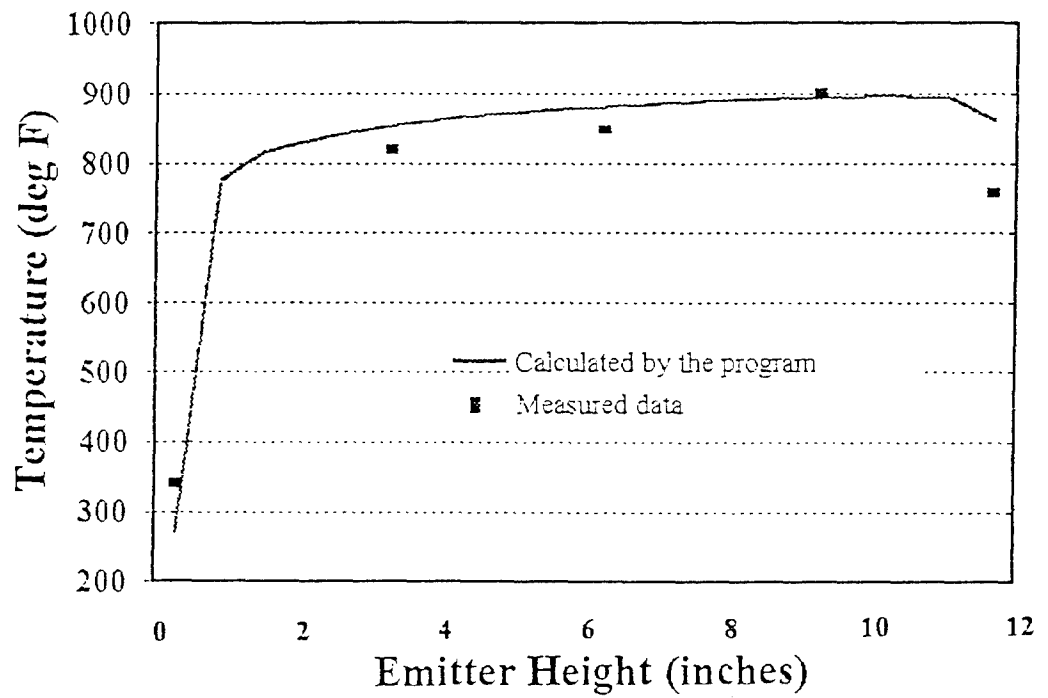
6. SHUT-DOWN:

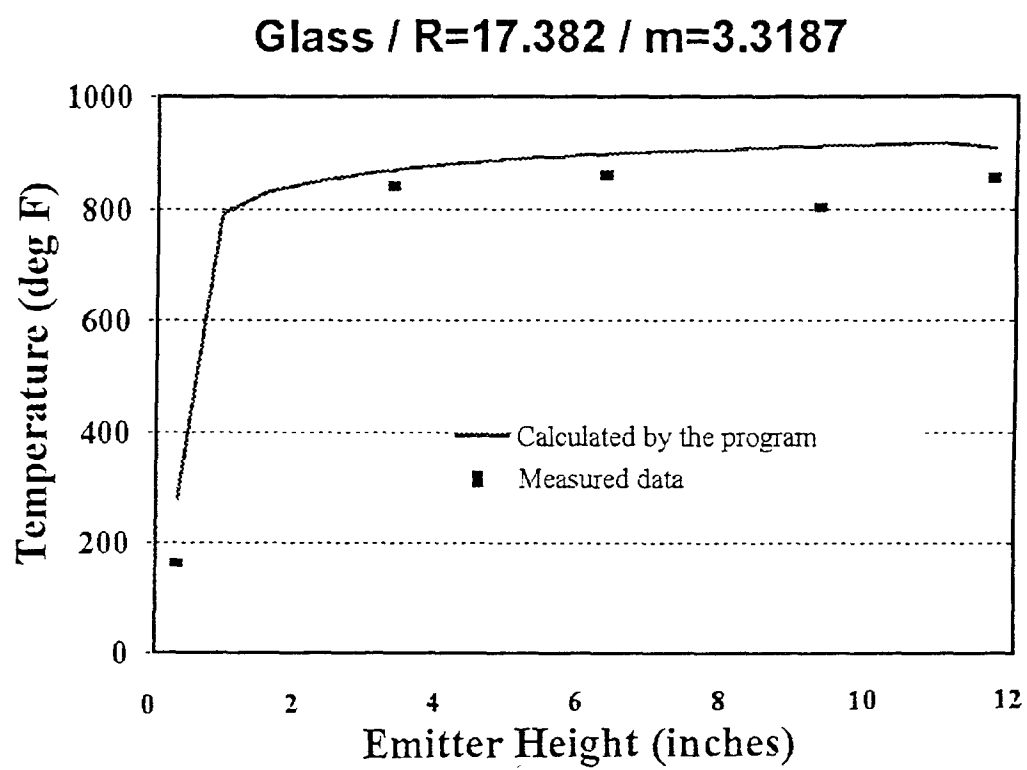
- ☐ Close valve VG-2 (CCW) and VG-3 (OL)
- ☐ Close valve VA-3 (CW) until FA-1 reads (10)
- ☐ Record pressure PG-1 _____
- ☐ Close valve VG-1 (CW)
- ☐ End data log, reset log file to c:\datadump and save setup
- ☐ Monitor temperatures until apparatus cools $< 200^{\circ}\text{F}$
- ☐ Close valve VA-3 (CCW)
- ☐ Record pressure VA-1 _____
- ☐ Close valve VA-1 (CCW)
- ☐ Shut off exhaust fan
- ☐ Secure area

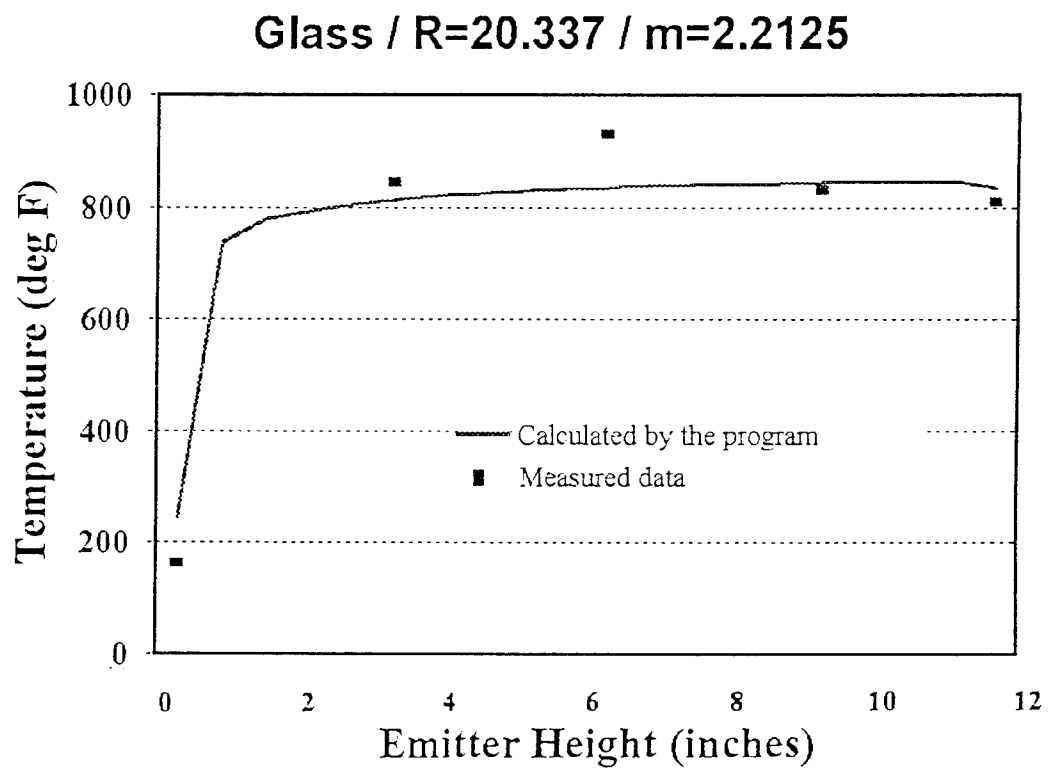
★EMERGENCY SHUT-OFF VALVE VG-3★

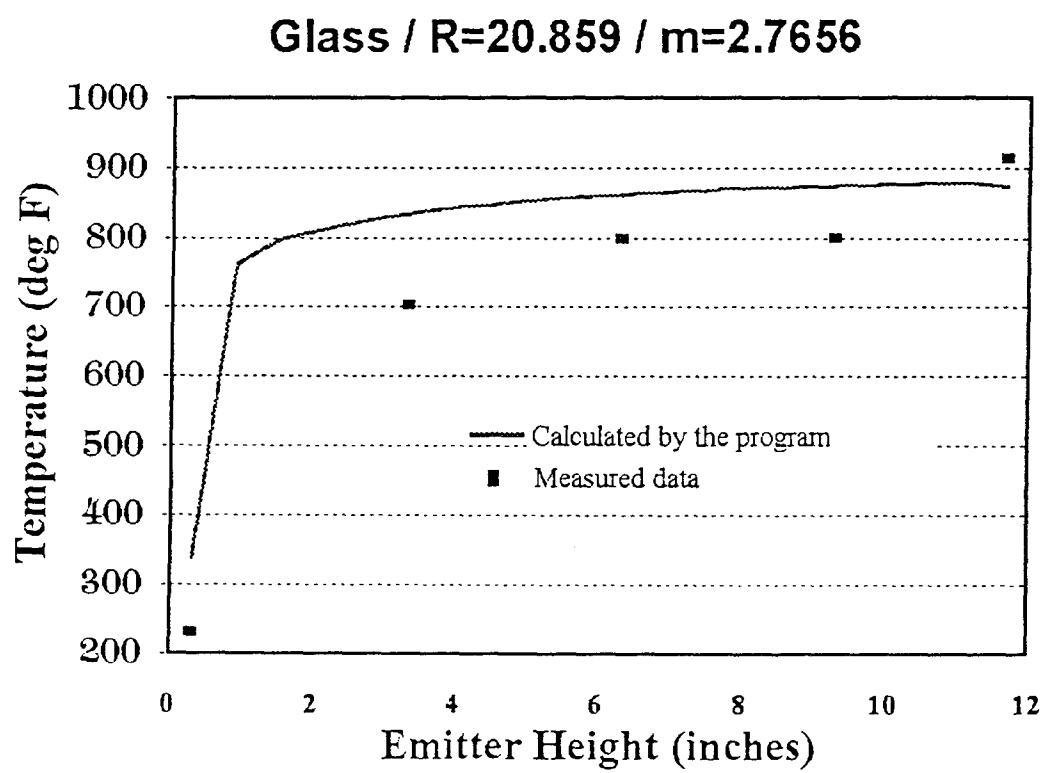
- Any Emergency or Unsafe Condition
- If Audible Temperature Alarm Sounds
- If FG-1 Ever Reads (0)

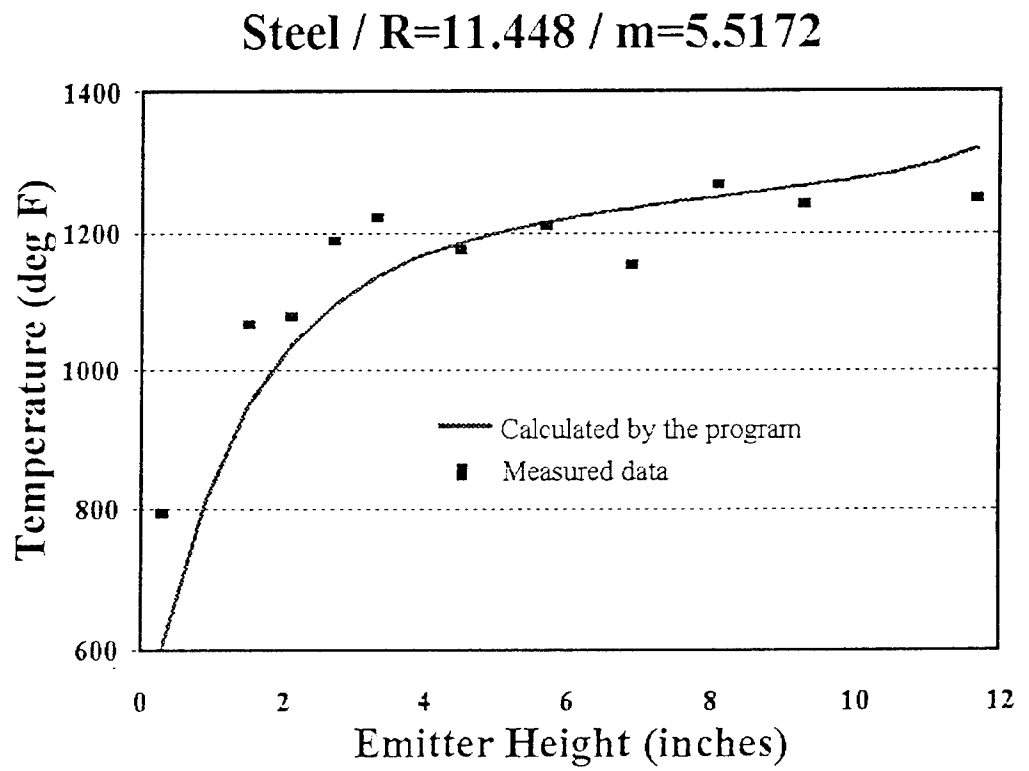
Glass / $R=13.906$ / $m=3.3187$



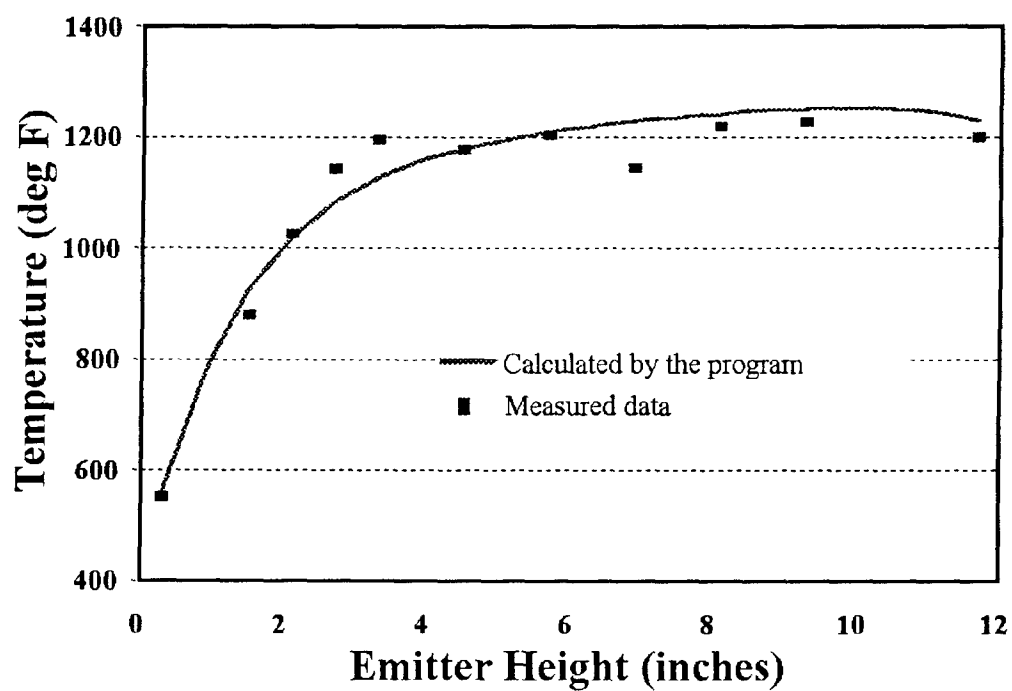


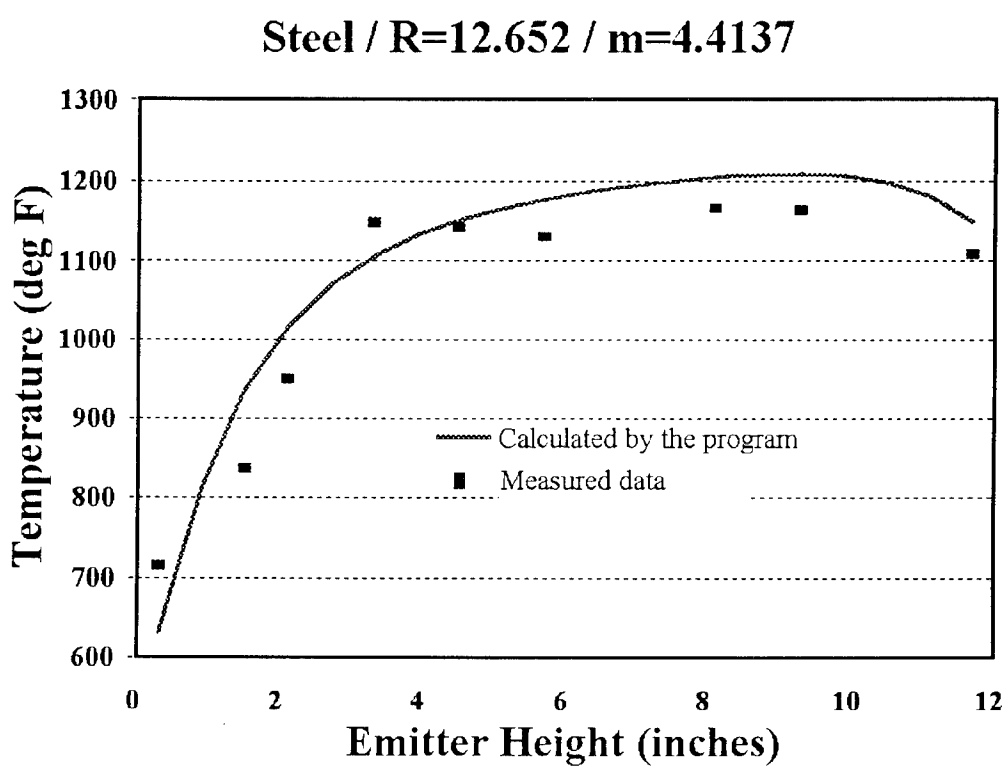




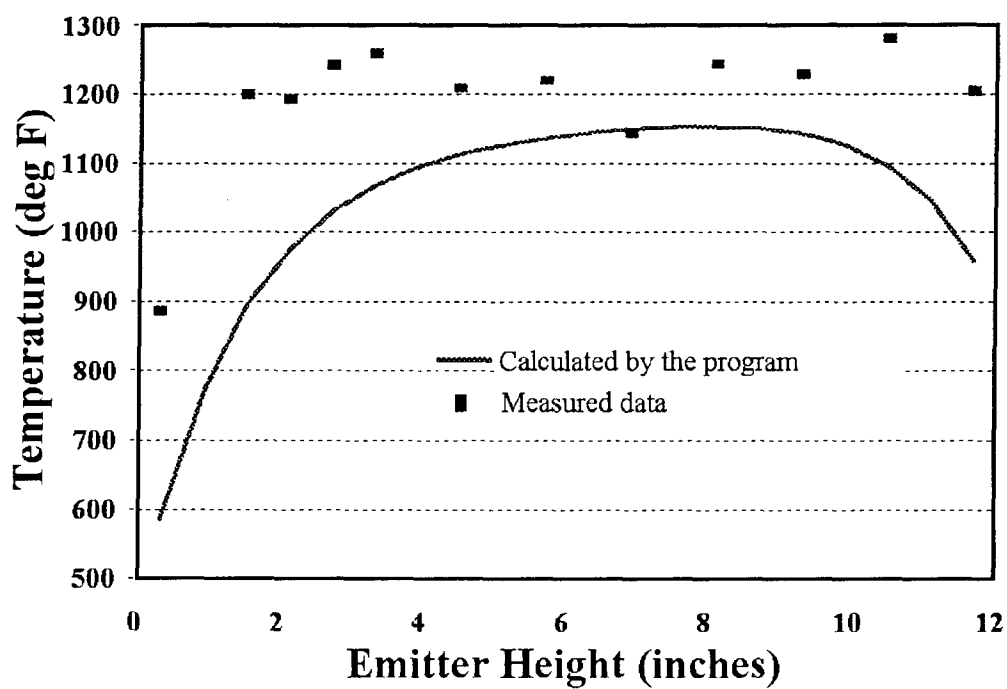


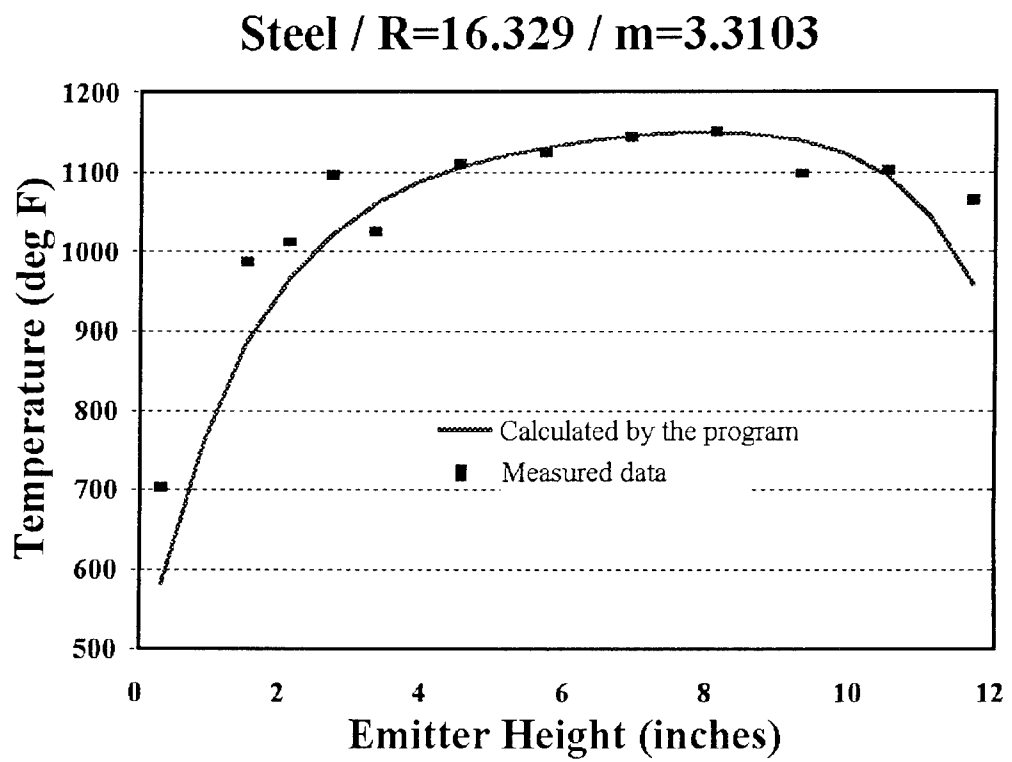
Steel / $R=12.101$ / $m=5.5172$



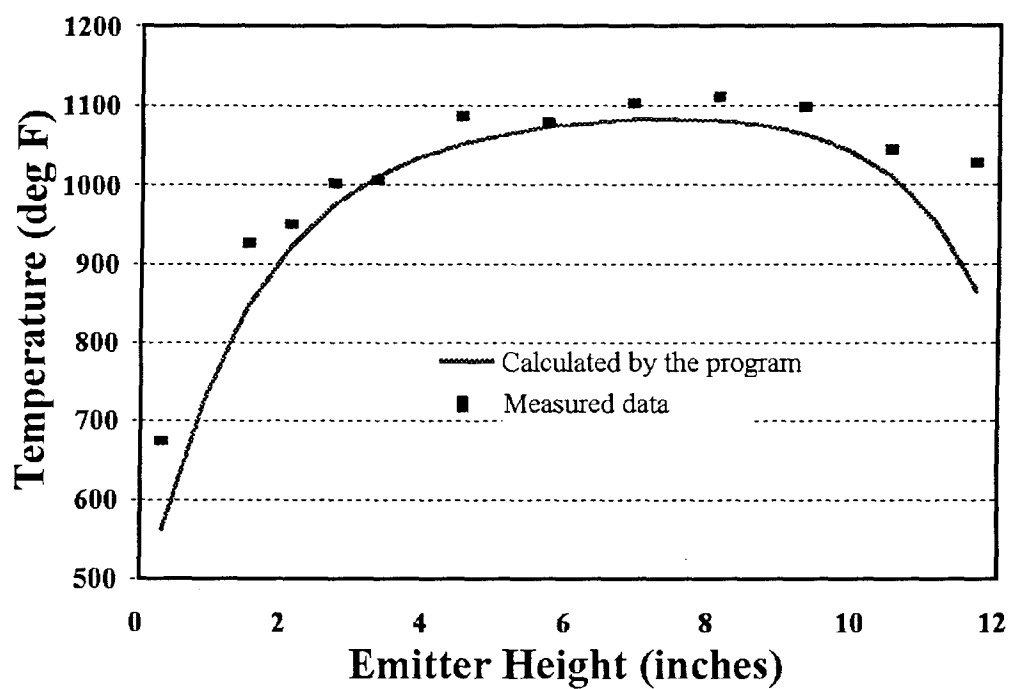


Steel / $R=13.941$ / $m=3.3103$

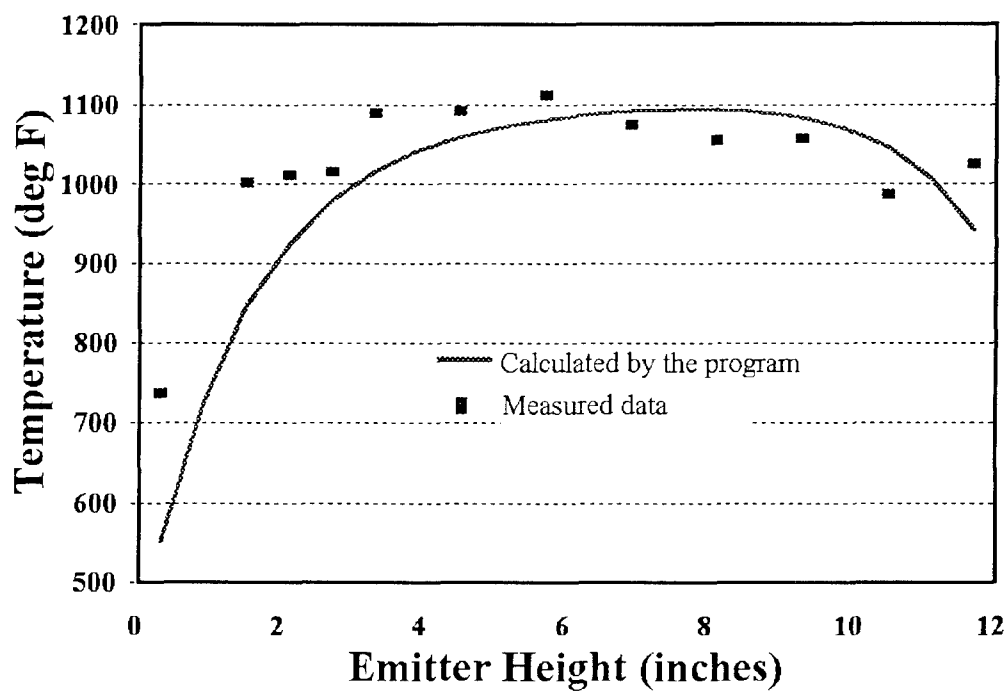




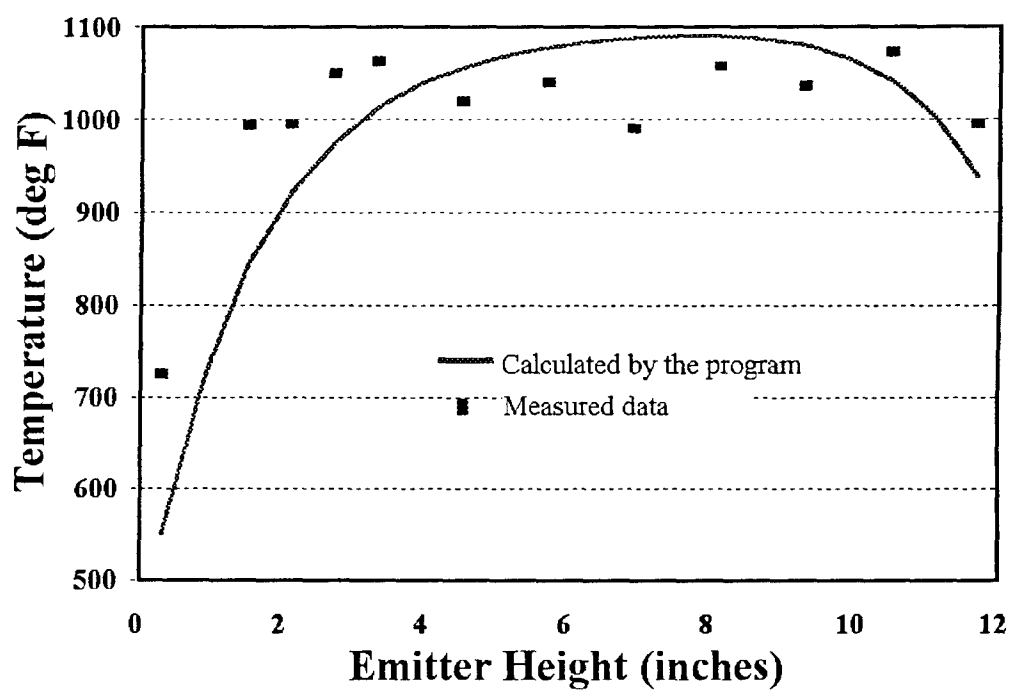
Steel / $R=17.421$ / $m=2.2069$

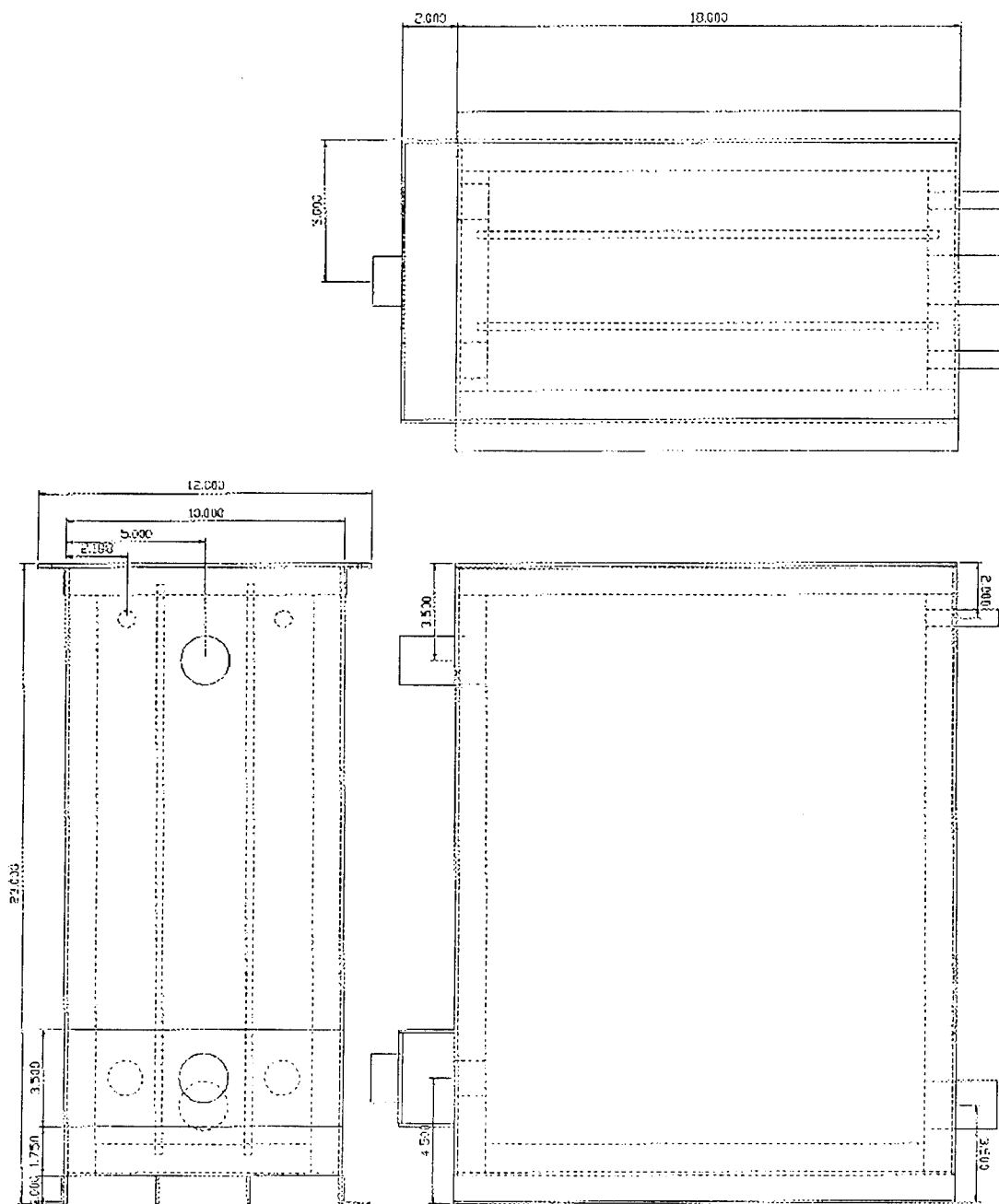


Steel / $R=19.915$ / $m=2.2785$



Steel / $R=20.912$ / $m=2.2069$





Heat Exchanger Design